Structures 32 (2021) 2004–2019

Contents lists available at ScienceDirect

Structures

journal homepage: www.elsevier.com/locate/structures

A simplified method to account for vertical human-structure interaction

K. Van Nimmen [a,*], A. Pavic [b,c], P. Van den Broeck [a]

[a] KU Leuven, Department of Civil Engineering, Structural Mechanics, B-3001 Leuven, Belgium
[b] College of Engineering, Mathematics and Physical Sciences, Vibration Engineering Section, University of Exeter, North Park Road, Exeter EX4 4QF, UK
[c] Full Scale Dynamics Ltd., Kay Building, North Park Road, Exeter EX4 4QF, UK

ARTICLE INFO

Keywords:
Human-induced vibrations
Human-structure interaction
Footbridge
Vibration serviceability

ABSTRACT

To account for vertical human-structure interaction (HSI) in the vibration serviceability analysis, the contact force between the pedestrian and the structure can be modelled as the superposition of the force induced by the pedestrian on a rigid surface and the force resulting from the mechanical interaction between the structure and the human body. For the case of large crowds, this approach leads to (time-variant) models with a very high number of degrees of freedom (DOFs). To simplify analysis, this paper investigates the performance of an equivalent single-degree-of-freedom approach whereby the effect of HSI is translated into an effective natural frequency and modal damping ratio for each mode of the supporting structure. First, the numerical study considers a footbridge structure that is modelled as a simply-supported beam for which only the fundamental vertical bending mode is taken into account. For a relevant range of structure and crowd parameters, the comparison is made between the structural response predicted by the simplified model and the more accurate reference model that accounts for all DOFs of the coupled crowd-structure model. Where the simplified model is found to underestimate the structural response, although to a limited extent, this is compensated for by introducing a correction factor for the effective damping ratio. Second, the performance of the simplified method is evaluated through the application on a real footbridge. The results show that the simplified method allows for a good and mildly conservative estimate of the structural acceleration response that is within 10–20% of the predictions of the reference crowd-structure model.

1. Introduction

Architects and engineers are designing ever more slender and lightweight footbridges. Being slender, these structures are sensitive to vibrations caused by the dynamic loading induced by pedestrians [1,2]. The point is now reached where the dynamic performance of these structures under high crowd densities has started governing their design. Recent studies [5,6] show that these human-structure interaction (HSI) effects, such as added damping, are in many cases a decisive factor when assessing the vibration serviceability of footbridges. Current design codes and guidelines, which pioneered the concept of crowd dynamic loading on footbridges, such as Sétra [3], HiVoSS [4] and the UK National Annex to Eurocode 1 [7], do not specify anything different than using the 'empty' modal properties of the footbridge, in particular damping. With such low 'empty' damping values, which are completely unwarranted for the crowd loading case, fairly standard beam-like footbridges spanning 30–40 m would need a considerable amount of tuned mass dampers (TMDs) to reduce the predicted excessive crowd-induced vibrations. Current implementation of state-of-the-art HSI methodologies to calculate a more realistic vibration response to crowd walking, e.g. [5,6], is quite expensive and requires specialist software to deal with non-proportionally damped systems. The consequent urgent need for a simplified procedure to account for HSI in engineering design practice is the main motivation for this work.

The walking behaviour of pedestrians can be considered as controlled by an internal driving force [8] and results into forces induced on the structure that supports them. On a perfectly rigid floor, these forces are equal to the well-known ground reaction forces (GRFs) as registered on a rigid laboratory floor [9]. These forces depend on the weight and the internal driving force of the pedestrian. On the other hand, when the supporting structure vibrates, so-called active and passive human-structure interaction phenomena (can) occur during walking:

- Active interaction phenomena, also called Structure-to–Human interaction (S2H) phenomena [10], imply that the internal driving

* Corresponding author.
E-mail address: katrien.vannimmen@kuleuven.be (K. Van Nimmen).

https://doi.org/10.1016/j.istruc.2021.03.090
Received 23 November 2020; Received in revised form 24 February 2021; Accepted 19 March 2021
Available online 22 April 2021

force of the pedestrian is modified, consciously or unconsciously, in response to the vibration of the surface. As a result, the pedestrian's walking behaviour and the induced forces are also modified [11–13]. These active interaction phenomena are known to result from lateral oscillations of the bridge deck [13–17]. As these interaction effects can significantly amplify the structural response [18,19], they should be accounted for in the vibration serviceability assessment (VSA) of footbridges that are sensitive to lateral human-induced vibrations. In the vertical direction, however, it is argued that active interaction phenomena only occur for vibration amplitudes that exceed the acceptable limits for vibration comfort [3,20]. In these cases, the pedestrians either stop walking or display a highly disturbed walking behaviour, both of which result in a significant reduction of the structural response [21]. It is for these reasons that these vertical active interaction phenomena are not further considered here.

- Passive interaction phenomena, also called Human-to-Structure (H2S) interaction phenomena [10], refer to the fact that the human body is a mechanical system that interacts with the supporting mechanical system. As a result, the dynamic behaviour of the coupled crowd-structure system can differ significantly from that of the empty structure, in particular for lightweight structures [6]. In the vertical direction, these passive HSI phenomena are much more frequent and relevant for the design practice [5,6].

In the literature, many studies have reported experimental evidence of these passive interaction effects. The most significant HSI effect is the effective modal damping ratios of the coupled crowd-structure system that are much higher than the inherent modal damping ratios of the empty structure [22–27]. In response to these observations, various numerical models have been proposed during the last decade to simulate these interaction effects. The most complex among these models are multibody (biomechanical) models, that easily use 30 or more degrees of freedom (DOFs) in combination with feedback and feedforward control algorithms to replicate the normal walking motion [28]. Also inspired by the literature in biomechanics are the inverted pendulum (IP) models [29–32]. For both multibody and IP models, experimental validation is lacking, in particular in view of simulating HSI effects, and the model complexity is considered too high for application in design practice.

The most common approach to describe the vertical HSI is to consider the pedestrian and the supporting structure as two linear subsystems that are coupled at a single contact point [6,27,33–35]. In this case, the contact force not only depends on the pedestrian's weight and internal driving force, but also on the dynamic behaviour of both subsystems (i.e. their relative motion). Assuming that there is no active HSI, allows decomposing the contact force in two independent terms: an autonomous force term independent of the vibrations of the supporting structure and an interaction term due to the mechanical interaction with the human body.A similar approach has been previously applied in the field of wind engineering [36,37] and building acoustics [38] to describe interaction phenomena.

For the present application, the autonomous force term corresponds to the well-known GRFs as registered on the rigid floor. Depending on the frequency range of interest, the mechanical system representing the human body is a single (SDOF) or multiple (MDOF) degree of freedom [39,40]. Concerning the vibration serviceability of footbridges, the frequency range of interest is typically between 0.5 and 6.0 Hz. In this frequency range, a good representation of the dynamic behaviour of the human body can be obtained by considering a SDOF model [6,27], for example the one presented in Fig. 1 (a): a sprung mass m_{h1}, an unsprung mass m_{h0}, a spring k_{h1} and damping element c_{h1}. Although the models proposed in the literature display small differences, they generally correspond in terms of the natural frequency (2.75–3.50 Hz) and the modal damping ratio (25–35%) of the human body model representing a pedestrian. [41] provides a more comprehensive overview of the experimental evidence and numerical models involving vertical HSI.

The objective of the this paper is to propose a new and simplified methodology for design practice that takes into account vertical HSI in the VSA of civil engineering structures occupied and dynamically excited by crowds. The state-of-the-art reference framework in this study simulates the vertical HSI for a single person by means of the SDOF model presented in Fig. 1 (a) with $f_{h1} = 3.25$ Hz, $\xi_{h1} = 0.30$ %, $m_h = m_{h1} + m_{h0} = 70$ kg and $\mu_{h1} = m_{h1}/m_h = 0.95$. However, as also stated in [6,41], these properties remain to be validated for large crowds and realistic loading conditions. To reflect on these uncertainties and keeping in mind that the impact of HSI is most sensitive to the ratio between the relevant natural frequency of the human body f_{h1} and the considered mode of the structure f_s, the results are also presented in terms of the dimensionless ratio f_{h1}/f_s. It is noted that even when future experimental studies indicate that these parameters need to be corrected, the presented methodology will still be valid as long as the low-frequency dynamic behaviour of the human body is highly damped and the distributions of f_{h1} and ξ_{h1} among the human population can be approximated by a Gaussian distribution. These are assumptions that can be made based on the currently available state of the art [41].

Concerning the crowd conditions, this study considers the conservative load case of (near-) resonance whereby the fundamental or second harmonic of the (near-) periodic walking load coincides with one of the natural frequencies of the occupied structure. Sparse [42,24] and dense [43,44] traffic conditions are represented by, respectively, a normal and low variability in step frequency between different pedestrians. This approach is in accordance to the one proposed by the design guides Sétra [3], HiVoSS [4] and the UK National Annex to Eurocode 1 [7]. The approach of these design guides is used because (1) it is specifically developed for engineering practice to assess the vibration serviceability of footbridges, (2) they are widely applied internationally and (3) the drafts of the next version of the Eurocodes propose to integrate this approach.

The outline of this paper is as follows. First, the reference crowd-structure model and the statistical approach to analyse the structural response are presented. Second, the simplified model is introduced. Then, the simplified model is verified as a good approximation of the reference model for the prediction of crowd-induced vibrations. Next, results reported in the literature are used for validation purposes. Finally, it is illustrated how the proposed simplified method can be integrated in general procedures for the VSA of footbridges. The procedure is then applied and its performance evaluated by application to a real footbridge with multiple modes in the frequency range of interest.

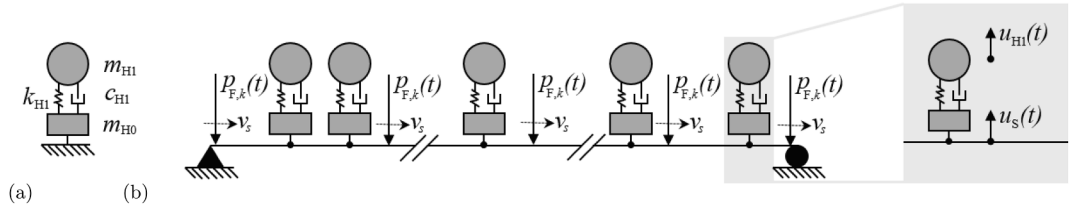

Fig. 1. The human body model (a) and the coupled crowd-structure model introduced in [6] (b).

2. The reference modelling framework

2.1. Governing equations

The crowd-structure model introduced in [6] is used in this study. The first-order continuous-time state-space equations of motion of the coupled moving crowd model read:

$$\dot{\mathbf{x}}(t) = \mathbf{A_c}\mathbf{x}(t) + \mathbf{B_c}\mathbf{S_p}(t)\mathbf{p_f}(t) \tag{1}$$

$$\text{with} \quad \mathbf{x}(t) = [\,\mathbf{z}(t) \quad \mathbf{u}_h(t) \quad \dot{\mathbf{z}}(t) \quad \dot{\mathbf{u}}_h(t)\,]^\top \tag{2}$$

with $\mathbf{x}(t) \in \mathbb{R}^{n_s}$ the modal state vector and $n_s = 2(n_m + n_h)$, $\mathbf{z}(t) \in \mathbb{R}^{n_m}$ the modal coordinate vector, n_m the number of modes, $\mathbf{p_f}(t) \in \mathbb{R}^{n_h}$ is the force vector collecting the time history of the autonomous force term $p_{f,k}(t)$ of each pedestrian k of the n_h pedestrians as rows and $\mathbf{S_p}(t) \in \mathbb{R}^{n_{dof} \times n_h}$ a selection matrix which transfers the forces to the corresponding n_{dof} DOFs of the model of the structure. The autonomous force term $p_{f,k}(t)$ is modelled using the probabilistic single-person force model developed by Živanović et al. [46]. The system matrices $\mathbf{A_c} \in \mathbb{R}^{n_s \times n_s}$ and $\mathbf{B_c} \in \mathbb{R}^{n_s \times n_{\text{dof}}}$ are defined as:

$$\mathbf{A_c} = \begin{bmatrix} \mathbf{0} & \mathbf{I} \\ -\overline{\mathbf{M}}_{hs}^{-1}\overline{\mathbf{K}}_{hs} & -\overline{\mathbf{M}}_{hs}^{-1}\overline{\mathbf{C}}_{hs} \end{bmatrix} \tag{3}$$

$$\mathbf{B_c} = \begin{bmatrix} \mathbf{0} \\ \mathbf{T_p} \end{bmatrix} \tag{4}$$

where $\overline{\mathbf{M}}_{hs}, \overline{\mathbf{K}}_{hs}$ and $\overline{\mathbf{C}}_{hs}$ are the generalised mass-, stiffness and damping matrices of the coupled crowd-structure system and $\mathbf{T_p}$ is the generalised input transformation matrix, as defined in [6].

2.2. Crowd characteristics

A crowd is characterised by inter- [47] and intra-person variability [9,48]. In [2] it is shown that the inter-person variability of the walking speed and the pedestrian weight have a negligible influence on the structural dynamic response [2]. Therefore, the weight $G = 700$ N [3,49] and walking speed v_s [m s^{-1}] are set equal to their mean value for all pedestrians. The walking speed is defined in terms of the pedestrian density d[pedestriansm^{-2}], as defined in [43,19]. The arrival times are set to follow a Poisson distribution [50,51]. The pedestrian's step frequency f_s and weight G characterise the vertical load exerted on a rigid floor, defined here by a probabilistic single-person force model (see Section 2.1).

In agreement with the methodology presented by the design guides Sétra [3] and HiVoSS [4], the conservative load case of (near-) resonant loading is of interest: the mean value of the step frequency f_p (or one of its integer multiples) is chosen to match one of the natural frequencies of the (occupied) structure f_{hs}. A distinction is made between low and high pedestrian densities:

- $d < 1$personsm^{-2} (sparse traffic): $f_s = \mathcal{N}(\mu_{f_s}, 0.175)$Hz [3,4]
- $1 \geqslant d \geqslant 1.5$personsm^{-2} (dense traffic): $f_s = \mathcal{N}(\mu_{f_s}, 0.05)$Hz [20]

with $1.0 < f_s < 2.5$ [20], f_p an integer multiple of the mean value of the step frequency μ_{f_s} and $\mathcal{N}$ representing a normal distribution.

The mechanical properties of the SDOF system used to simulate the passive interaction between the pedestrian and the structure are set to approximate the low-frequency dynamic behaviour of the human body during the walking cycle. It is shown in [6] that the impact of the inter-person variability on the parameters of the human body models is low. Therefore, only the mean values ($f_{h1} = 3.25$Hz, $\xi_{h1} = 0.30$ [6,27,40]) are considered here.

2.3. Statistical analysis

Given the statistical nature of pedestrian excitation, the structural response is best evaluated by means of a statistical analysis [52,42]. In this study, the structural response is evaluated by Monte Carlo simulation considering the variability of the autonomous force term $\mathbf{p_f}(t)$. For each sample of the Monte Carlo process, the maximum acceleration level over the relevant observation time window with length T is determined, with T [s] denoting the time needed by a pedestrian to cross the bridge span with length L [m] ($T = L/v_s$), where v_s, and thus also T, is the same for all pedestrians (Section 2.2). In agreement with [3,4], the output quantity of interest concerns the 95 percentile value of the maximum acceleration levels. The number of Monte Carlo samples is increased until the probability that the true percentile of the distribution is within ±5% of the corresponding percentile of the simulated data accumulated until that point, is higher than 95% (Matlab Statistics Toolbox, [53]). A more comprehensive discussion of this approach and an illustrative example can be found in [54].

3. Simplified model

To simplify analysis, this study introduces an equivalent model whereby the effect of passive HSI is translated into effective (or 'apparent') modal parameters for each mode of the supporting structure. In other words, these effective modal parameters are introduced to represent the dynamic behaviour of the coupled crowd-structure system. The simplified model is a very reasonable and cost effective alternative for the reference coupled crowd-structure model presented in Section 2.1: The model order is reduced from $n_s = 2(n_m + n_h)$ to $2n_m$. Given the fact that the number of modes n_m representing the structure is generally limited and much smaller than the number of pedestrians n_h, the model order can be significantly reduced. Similar effective parameters have been investigated in recent studies [6,27,45].

The motivation for this simplified model stems from the resemblance between the dynamic behaviour of the coupled crowd-structure system and that of the empty structure. The dynamic behaviour of the coupled crowd-structure system is examined based on its accelerance frequency response function (FRF) $H_{hs}(\omega)$ [6] for an input force and output acceleration at the antinode of a given structural mode, found using the system transfer function for the linear state-space model introduced in Section 2.1. For the empty structure, the FRF (H_s) only depends on the modal characteristics of the empty structure.

Consider the empty structure. It can be assumed that for (near-) resonant excitation of mode j, the contribution of mode j dominates the structural response. As in the remainder of this section only the (near-) resonant mode j of the structure is retained, the subscript j is omitted when referring to the corresponding natural frequency f_s, modal damping ratio ξ_s, unity-normalised mode shape Φ_s and modal mass m_s [55]. The maximum steady-state amplitude of the single-mode response of the empty structure ($\ddot{u}_{s,\max}$) is found for resonant loading at the antinode ($\max|\Phi_s| = \boldsymbol{1.0}$) of the resonant mode:

$$\ddot{u}_{s,\max} = p_0 \max_\omega |H_s(\omega)| = p_0 |H_s(\omega_s)| = \frac{p_0}{2\xi_s m_s} \tag{5}$$

$$\text{with} \quad f_s = \frac{\omega_s}{2\pi}\sqrt{1 - 2\xi_s^2} \tag{6}$$

with p_0 [N] the amplitude of the sinusoidal input, ω_s the acceleration resonant frequency and f_s the undamped resonant natural frequency [56]. Eq. (5) shows that the key structural parameters determining its dynamic response are the natural frequency f_s, the modal damping ratio ξ_s and the modal mass m_s.

It is shown in [6] and illustrated in Fig. 2 for different ratios between the total mass of the crowd ($m_{cr} = n_h m_h$) and the structure (m_{str}), that both the FRF of the empty structure and the FRF of the coupled crowd-structure system are characterised by a single peak. This behaviour is the

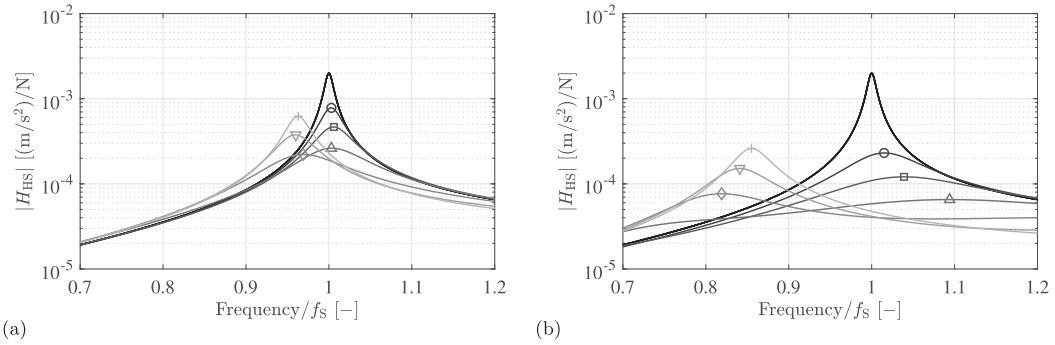

Fig. 2. The modulus of the accelerance FRF $H_{hs}(\omega)$ of the coupled crowd-structure system with $\xi_s = 0.5\%$, for a frequency ratio f_{h1}/f_s of: 0.4 (∘), 0.6 (□), 0.8 (△), 1.0 (⋄), 1.2 (▽) and 1.4 (+) and of the empty structure (black), for a mass ratio m_{cr}/m_{str} of (a) 0.05 and (b) 0.25..

same as that of a tuned mass damper, with a damping ratio significantly higher than the optimum damping ratio [57,58]. The peak value of the FRF $H_{hs}(\omega)$ can be considered as a measure for the maximum amplitude of the steady-state acceleration response of the coupled crowd-structure system ($\ddot{u}_{hs,\max}$) exposed to resonant harmonic excitation with amplitude p_0:

$$\ddot{u}_{hs,\max} = p_0|H_{hs}(\omega_{hs})| = \frac{p_0}{2\xi_{\text{eff}}m_{\text{eff}}}, \tag{7}$$

$$\text{with } \omega_{hs} = \text{argmax}_{\omega}|H_{hs}(\omega)| \tag{8}$$

$$f_{\text{eff}} = \frac{\omega_{hs}}{2\pi}\sqrt{1-2\xi_{\text{eff}}^2} \tag{9}$$

where f_{eff} [Hz], ξ_{eff} [-], and m_{eff} [kg] are defined as the (undamped) 'effective natural frequency', 'effective damping ratio' and 'effective mass' of the coupled crowd-structure system. In this study, the assumption is made that the effective mass is equal to the modal mass of the empty structure:

$$m_{\text{eff}} = m_s \tag{10}$$

This choice is made to keep the methodology as simple as possible by using two effective parameters, instead of three (i.e. similar to the approach adopted in [59]). In addition, this modelling choice implies that the mode shapes of the equivalent coupled crowd-structure system are identical to those of the empty structure. The mass-effect of the crowd is thus taken into account by both the change in the effective damping ratio and effective natural frequency. However, it is noted that this is only valid at (near-) resonance, which is the main concern of design calculations when checking vibration serviceability. In summary, the presented methodology accounts for the mass, damping and stiffness effects by means of the effective natural frequency f_{eff} and effective damping ratio ξ_{eff} of the coupled crowd-structure system at (near-) resonance.

The limitation of the proposed methodology is that it assumes that the dynamic properties of the coupled crowd-structure system can be well-approximated by a time-invariant system. This assumption is valid when the position of the humans is time-invariant, e.g. for grandstand applications, and was validated in [6] for the application to footbridges for pedestrian densities of 0.2 personsm^{-2} and higher. In the latter case, the crowd can be considered (roughly) homogeneous and uniformly distributed over the bridge deck. Although the proposed methodology is in this paper applied to the specific case of footbridges, the methodology itself is applicable to both moving and stationary dynamic excitation, as long as (near-) resonant excitation is of interest and the human SDOF parameters are known.

4. Numerical study

The characteristics of the simplified model (the effective modal parameters of the coupled crowd structure system) are determined for a realistic range of structure and crowd parameters. In addition, this section validates the simplified model as a good approximation of the reference crowd structure system (Section 2.1) when the (near-) resonant structural response to pedestrian excitation is of interest. To this end, the structural response predicted by both models is compared using a realistic range of structure and crowd parameters.

4.1. Input parameters

aaa

- Structure parameters: The dynamic behaviour of the structure, with total mass m_{str}, is represented by the modal parameters of the resonant mode $j: f_{sj}, \Phi_{sj}, \xi_{sj}$ and m_{sj}. As footbridges are generally lowly-damped, modal damping ratios ξ_{sj} between 0.2% and 2.0% are considered. In view of the vibration serviceability issues of footbridges, the natural frequency is varied between 1 Hz and 6 Hz [3,4]. A single vertical bending mode is considered with a half-sine mode shape and $m_{sj} = \frac{1}{2}m_{str}$, as for a simply supported beam. No range is specified for the modal mass m_{sj} but a reasonable range is considered for the ratio between the total crowd (m_{cr}) and total bridge mass (m_{str}). The structural mass of footbridges is generally found to be between 350 kg and 1000 kg per m^2 of the bridge deck. A maximum pedestrian density of 1.5 pedestriansm^{-2} then corresponds on average to $1.5 \times 70 = 105$kgm^{-2}, which therefore corresponds to an upper limit of the crowd to structure mass ratio of about 30% ($m_{cr}/m_{str} = 105/350 \approx 0.3$).
- Crowd characteristics: The human body model parameters are set to their mean value (see Section 2.2): $m_h = 70$ kg [49] and $m_{h1} = 0.95m_h, m_{h0} = 0.05m_h, f_{h1} = 3.25$Hz, $\xi_{h1} = 0.30$. As at this point the mass ratio is specified rather than the pedestrian density, the structural response is predicted considering both sparse and dense traffic conditions (Section 2.2).

The following non-dimensional quantities are introduced:

$$\overline{f}_{j\text{eff}} = f_{j\text{eff}}\Big/f_{sj} \tag{11}$$

$$\overline{\xi}_{j\text{eff}} = \xi_{j\text{eff}}\Big/\xi_{sj} \tag{12}$$

$$\overline{f}_j = f_{h1}\Big/f_{sj} \tag{13}$$

$$\overline{m}_j = \frac{m_{j,\mathrm{add}}}{m_{sj}} \text{ with } m_{j,\mathrm{add}} = \rho \int\int_{L_x L_y} \Phi_{sjv}^2\left(x,y\right)\mathrm{d}x\mathrm{d}y \tag{14}$$

with $\overline{f}_{j\mathrm{eff}}$ and $\overline{\xi}_{j\mathrm{eff}}$ respectively the normalised effective natural frequency and damping ratio for mode j of the empty structure, $\overline{f}_j$ the ratio between the natural frequency of the human body model and the natural frequency of mode j of the empty structure, and $\overline{m}_j$ the ratio between the modal mass ($m_{j,\mathrm{add}}$ [kg]) added by the crowd with ρ [kgm^{-2}] the crowd mass per unit area, and the modal mass of mode j of the empty structure, with $\Phi_{sjv}(x,y)$ denoting the vertical component of the unity-normalised modal displacements at location (x,y) on the surface of the structure L_xL_y. The formulation in Eq. (14) can be used for any mode shape.

Given the above specified ranges for f_{sj} and f_{h1}, a lower and upper bound of approximately 0.5 and 3.5 respectively is found for $\overline{f}_j$. To account for the uncertainty that remains on f_{h1}, the range considered for $\overline{f}_j$ is widened to: $0.25 < \overline{f}_j < 6$. For the special case of a sinusoidal mode shape and a modal mass equal to half of the total mass of the structure, the upper bound of the mass ratio $\overline{m}_j$ is 0.3.

4.2. Output quantities of interest

aaa

- Effective modal parameters: the normalised effective natural frequency $\overline{f}_{\mathrm{eff}j}$ and damping ratio $\overline{\xi}_{\mathrm{eff}j}$.
- 95 percentile value of the maximum acceleration levels: calculated according to the reference crowd-structure model ($\ddot{u}_{HSI95}$) and the simplified model ($\ddot{u}_{\mathrm{eff}95}$), considering the statistical approach detailed in Section 2.3. The following ratio is defined:

$$R_{\mathrm{eff}} = \frac{\ddot{u}_{\mathrm{eff}95}}{\ddot{u}_{HSI95}} \tag{15}$$

R_{eff} greater (less) than unity indicates that the simplified model ($\ddot{u}_{\mathrm{eff}95}$) overestimates (underestimates) the response predicted by the reference model ($\ddot{u}_{HSI95}$).

4.3. Results

Fig. 3 compares the modulus and phase angle of the FRF of the reference coupled system and the simplified model for a mass ratio $\overline{m}_j$ of 0.05 and 0.25, and for different frequency ratios $\overline{f}_j = \{0.4, 0.6, 0.8, 1.0, 1.2, 1.4\}$.Similar to the reference coupled crowd-structure system, the FRF of the simplified model is found using its system matrices which are in this case composed solely of the effective modal parameters. Table 1 lists the relative difference ε between the modulus of the FRF of the reference crowd-structure model (H_{hs}) and the simplified model ($\widehat{H}_{hs}$), calculated as:

$$\varepsilon = \frac{\left|\widehat{H}_{\mathrm{hs}} - H_{\mathrm{hs}}\right|}{|H_{\mathrm{hs}}|}\,\mathrm{sgn}\left(\left|\widehat{H}_{\mathrm{hs}}\right| - \left|H_{\mathrm{hs}}\right|\right) \tag{16}$$

where the sign function (sgn) introduces a negative sign for the cases of underestimation, where the FRF modulus of the simplified model is for the most part below its coupled crowd-structure system counterpart. This relative error is evaluated over different frequency ranges, considered relevant for (near-) resonant excitation: $\pm 2.5\%\overline{f}_{\mathrm{eff}j}$, $\pm 5\%\overline{f}_{\mathrm{eff}j}$, $\pm 10\%\overline{f}_{\mathrm{eff}j}$ and $\pm 15\%\overline{f}_{\mathrm{eff}j}$. For $f_{\mathrm{eff}j} = 2$ Hz, these ranges approximate the frequency band in which 70% ($1\times\sigma$) to 95% ($2\times\sigma$) of the spectrum of the load is expected, for both sparse ($\mathcal{N}(\mu_{f_p}, 0.175)$, $\pm 10\%\overline{f}_{\mathrm{eff}j}$ and $\pm 15\%\overline{f}_{\mathrm{eff}j}$) and dense ($\mathcal{N}(\mu_{f_p}, 0.05)$, $\pm 2.5\%\overline{f}_{\mathrm{eff}j}$ and $\pm 5\%\overline{f}_{\mathrm{eff}j}$) traffic conditions.

Fig. 3 shows that (small) modelling errors become apparent in the form of (small) differences in both amplitude and phase as the excitation frequency is further away from the resonant frequency of the coupled system. These differences increase for increasing mass ratios (Figs. 3-c vs a, and 3-d vs b) but altogether remain limited. These differences result from the fact that the simplified model is introduced to translate the

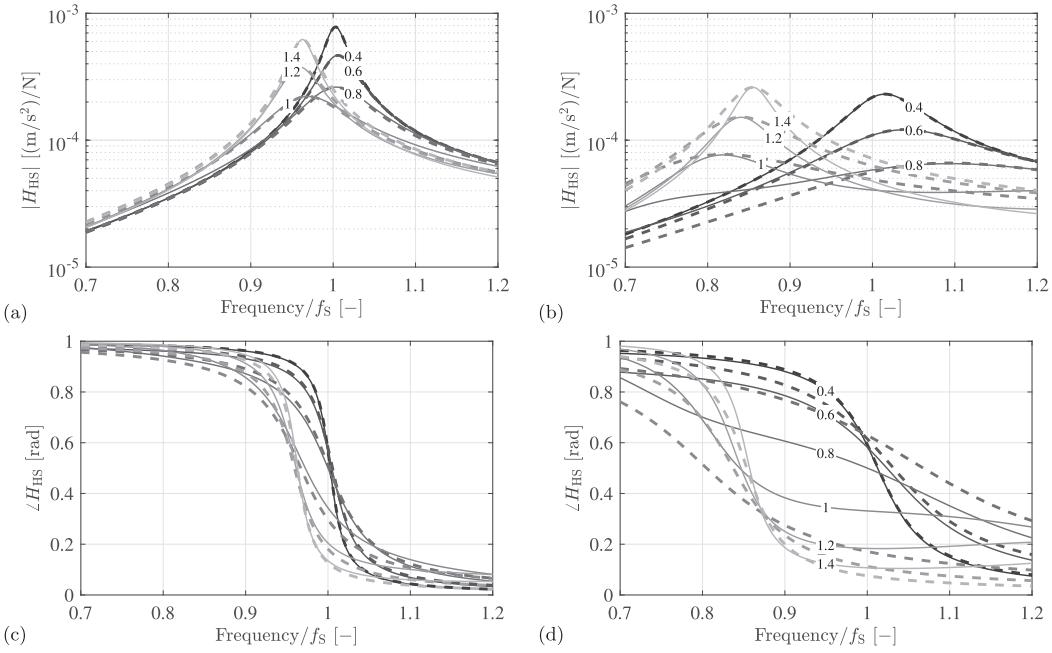

Fig. 3. The modulus (a,b) and phase angle (c,d) of the accelerance FRF $H_{hs}(\omega)$ of the coupled crowd-structure system calculated based on the reference system (solid) and the simplified model (dashed) for $\xi_s = 0.5\%$, a mass ratio $\overline{m}_j$ of (a,c) 0.05 and (b,d) 0.25, and for increasing frequency ratios $\overline{f}_j$ (dark to light): 0.4, 0.6, 0.8, 1.0, 1.2 and 1.4.

Table 1
The relative difference in the modulus of the FRF of the coupled crowd-structure system and the FRF of the simplified model (ε) over a frequency range of $\pm 2.5\%\bar{f}_{\mathrm{eff}j}$, $\pm 5\%\bar{f}_{\mathrm{eff}j}$, $\pm 10\%\bar{f}_{\mathrm{eff}j}$ and $\pm 15\%\bar{f}_{\mathrm{eff}j}$, for frequency ratios ($\bar{f}_j$) 0.4, 0.6, 0.8, 1.0, 1.2 and 1.4, and the mass ratios ($\overline{m}_j$) 0.05 and 0.25.

	$\overline{m}_j = 0.05$				$\overline{m}_j = 0.25$			
$\bar{f}_j$	$\pm 2.5\%\bar{f}_{\mathrm{eff}j}$	$\pm 5\%\bar{f}_{\mathrm{eff}j}$	$\pm 10\%\bar{f}_{\mathrm{eff}j}$	$\pm 15\%\bar{f}_{\mathrm{eff}j}$	$\pm 2.5\%\bar{f}_{\mathrm{eff}j}$	$\pm 5\%\bar{f}_{\mathrm{eff}j}$	$\pm 10\%\bar{f}_{\mathrm{eff}j}$	$\pm 15\%\bar{f}_{\mathrm{eff}j}$
0.40	−0.81	−0.80	−0.77	−0.76	0.23	0.29	0.30	0.29
0.60	−0.72	−0.79	−0.80	−0.79	0.31	0.25	−0.37	−0.61
0.80	−0.80	−1.78	−2.72	−3.08	1.11	0.93	1.28	−3.07
1.00	−0.75	−1.90	−3.31	−4.08	2.69	7.06	15.27	19.49
1.20	2.30	3.75	4.57	4.76	5.71	13.50	21.81	25.22
1.40	3.93	5.18	5.81	6.00	9.59	17.17	22.54	24.48

dominant effect of HSI in effective modal parameters (f_{eff} and ξ_{eff}) for each mode of the supporting structure. This is a modelling choice that reduces the model order from $n_s = 2(n_m + n_h)$ to $2n_m$ and inevitably involves approximations. The effective modal parameters are defined such that they accurately represent the dynamic behaviour of the coupled system at resonance. As the simplified model is developed for civil engineering structures occupied and dynamically excited by crowds, it is exactly this (near-) resonant behaviour of the coupled system that is of interest. It is for this reason that the modelling errors emerging away from resonance are of little importance in the proposed methodology. These results furthermore show that in terms of amplitude, away from resonance the FRF modulus of the simplified model is in most cases (slightly) greater than the FRF modulus of the reference crowd-structure system. In other words, the simplified model is on the safe side for non-resonant excitation. Only when both $\bar{f}_j \lesssim 1$ and the frequency range below the resonant frequency of the coupled system are considered, the amplitude of the FRF modulus of the simplified model is found to be (slightly) smaller than the modulus of the reference system (see Fig. 3-b). For these cases, the simplified model is not on the safe side for non-resonant excitation. At the end of this section, it is discussed how this issue is addressed for (near-) resonant excitation by crowds by the introduction of a correction coefficient.

The above observations are confirmed and more clearly represented

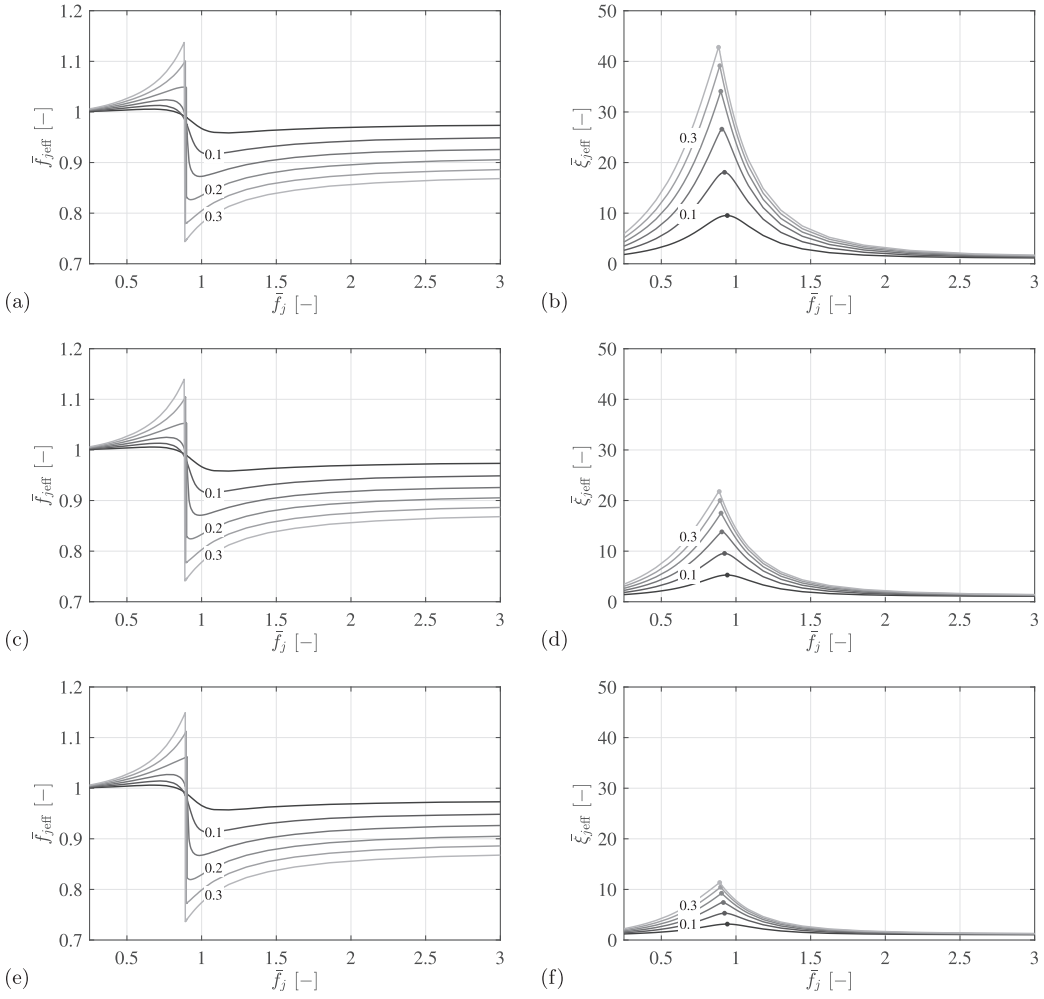

Fig. 4. The normalised effective natural frequency $\bar{f}_{j\mathrm{eff}}$ (a,c,e) and normalised effective damping ratio $\bar{\xi}_{j\mathrm{eff}}$ (b,d,f) of the coupled crowd-structure system for the normalised mass ratios $\overline{m}_j = \{0.05, 0.10, 0.15, 0.20, 0.25, 0.30\}$and a structure with a modal damping ratio ξ_s of 0.5% (a,b), 1.0% (c,d) and 2.0% (e,f), in terms of the normalised natural frequency $\bar{f}_j$, and corresponding frequency for which f_{h1} is optimally tuned (•, Eq. (17)).

by the results in Table 1: The relative difference ε generally increases as the FRF moduli are compared over a greater range around the resonant frequency. For a mass ratio of 0.25, ε is between -3 % underestimation and $+25$ % overestimation, respectively.

Fig. 4 presents the normalised effective natural frequency $\bar{f}_{\mathrm{eff}j}$ and normalised effective damping ratio $\bar{\xi}_{\mathrm{eff}j}$ in terms of the normalised natural frequency $\bar{f}_j$, for the modal damping ratios $\xi_j = \{0.5, 1.0, 2.0\}$ and the normalised mass ratios $\bar{m}_j = \{0.05, 0.10, 0.15, 0.20, 0.25, 0.30\}$. To complement these dimensionless results and considering a natural frequency of the human body model f_{h1} of 3.25 Hz, Fig. 5 presents the effective natural frequency $\bar{f}_{\mathrm{eff}j}$ and effective damping ratio $\xi_{\mathrm{eff}j}$ in terms of the natural frequency of mode j of the empty structure. These figures aim to illustrate how these graphs and results can be used in engineering practice (as illustrated in Section 5). For reasons of readability, again, the normalised effective natural frequency $\bar{f}_{\mathrm{eff}j}$ is displayed. Together, Figs. 4 and 5 represent the effective quantities for the wide range of low-frequency modes of any empty footbridge, with a natural frequency between 1 and 6 Hz and modal damping ratios up to 2%. The following observations are made:

- For high values of the normalised natural frequency ($\bar{f}_j > 1.5$), the effect of the human presence is similar to that of an equivalent added mass: the effective natural frequency reduces in relation to the mass ratio and the effective damping ratio is approximately equal to the modal damping ratio of the empty structure ($\xi_{\mathrm{eff}j} \approx \xi_{sj}$) [6,60].
- For intermediate values of the normalised natural frequency ($0.5 < \bar{f}_j < 1.5$), the most significant HSI effect is in the increase in the effective damping ratio relative to the one of the empty structure [6,41,60]. Similar to the behaviour of a tuned mass damper, the highest effective damping ratio is found for frequency ratios $\bar{f}_j$ (slightly) below unity, corresponding to the optimal tuning frequency for accelerations [57,58,61]:

$$f_{opt} = \frac{1}{\sqrt{1+\bar{m}_j}} f_{sj} \tag{17}$$

Figs. 5 b,d,f show that regardless of the inherent structural damping, similar values for the effective damping ratio of the coupled crowd-structure system are obtained. This observation indicates that, relative to the low structural damping, the damping introduced by the crowd is dominant.

- For low values of the normalised natural frequency ($\bar{f}_j < 0.5$), the effective damping ratio again increases with the mass ratio, but less strong than for intermediate natural frequencies [6].
- It can be observed that the effective natural frequency is slightly lower (for $f_{sj} < f_{opt}$) or higher (for $f_{sj} > f_{opt}$) than the natural frequency of the empty footbridge [60,62,63]. The trends are highly similar for modal damping ratios up to 2%.

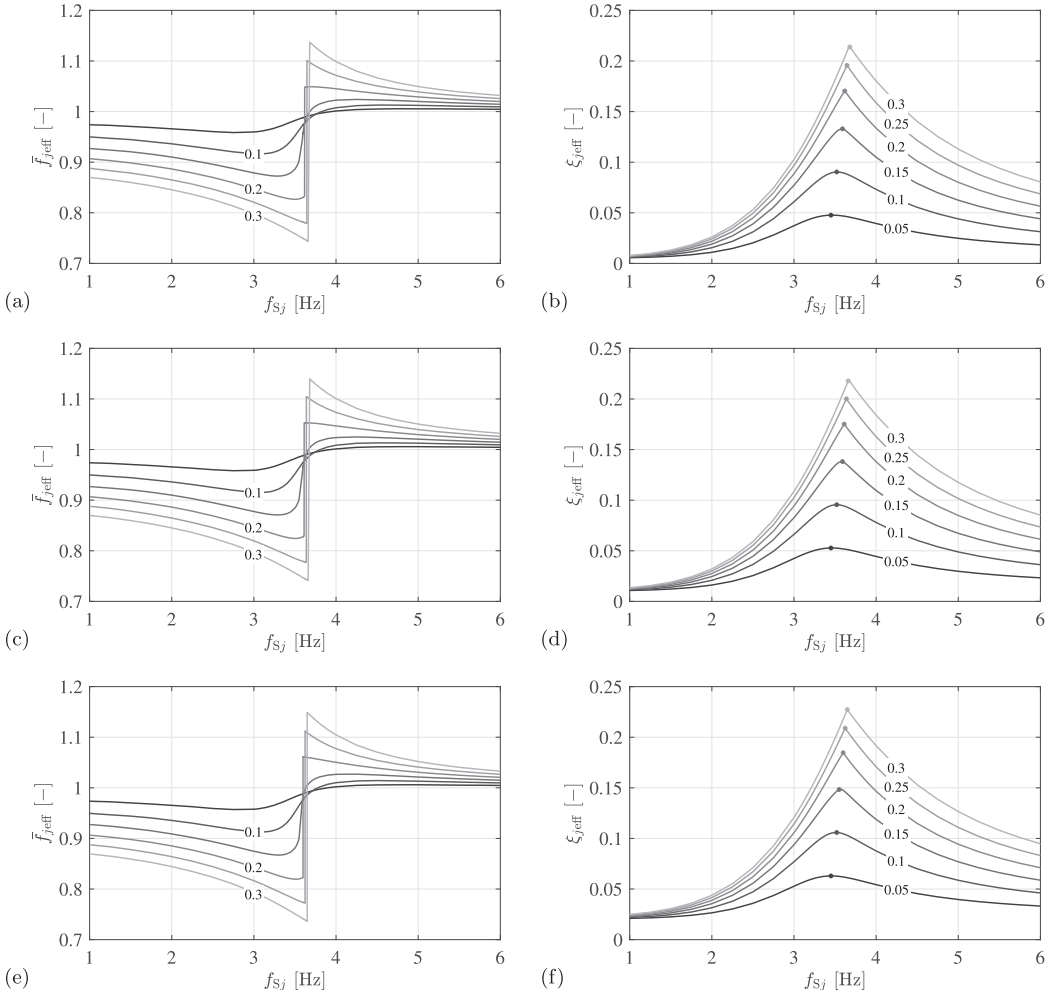

Fig. 5. The normalised effective natural frequency $\bar{f}_{j\mathrm{eff}}$ (a,c,e) and the effective damping ratio $\bar{\xi}_{j\mathrm{eff}}$ (b,d,f) of the coupled crowd-structure system for the normalised mass ratios $\bar{m}_j = \{0.05, 0.10, 0.15, 0.20, 0.25, 0.30\}$and a structure with a modal damping ratio ξ_s of 0.5% (a,b), 1.0% (c,d) and 2.0% (e,f), in terms of the natural frequency of mode j of the empty structure, and corresponding frequency for which $f_{h1} = 3.25$ Hz is optimally tuned (•, Eq. (17)).

- For the three widely ranging values of structural damping values for a typical normal footbridge (0.5%, 1% and 2%), Figs. 4 and 5 indicate little effect of the structural damping on the normalised effective natural frequency and damping ratio.

Next, focus is on the ratio R_{eff} between the structural acceleration response predicted by the reference crowd-structure model and the simplified model. Fig. 6 presents the ratios R_{eff} in terms of the natural frequency of the empty structure (f_{sj}), for the normalised mass ratios $\overline{m}_j = \{0.05, 0.10, 0.15, 0.20, 0.25, 0.30\}$ and two values of the modal damping ratio $\xi_{sj} = \{0.5, 2.0\}$ %. This figure shows that the ratios R_{eff} are close to unity. These results suggest that the structural response predicted by the reference crowd-structure system and the simplified model are comparable. For natural frequencies of the empty structure (f_{sj}) lower and higher than f_{opt} (Eq. 17), the simplified model respectively overestimates and underestimates the structural response. The difference in the predictions increases with the mass ratio. Note that when $f_h = 3.25$ Hz, the human body models are optimally tuned for natural frequencies of the empty structure close to 3.33 Hz and 3.71 Hz for normalised mass ratios $\overline{m}_j$ ranging from 0.05 to 0.30. For a mass ratio $\overline{m}_j = 0.3$, the structural response is overestimated by approximately 25%. The largest underestimation is found for natural frequencies of the empty structure near 4 Hz. For the mass ratio $\overline{m}_j = 0.3$, the structural response is underestimated by approximately 20%.

The differences between the predictions of the reference crowd-structure system and the simplified model stem from the fact that the simplified model allows for a good but not perfect representation of the dynamic behaviour of the reference crowd-structure system. As previously observed in Fig. 3, a nearly perfect fit is obtained for the most important (near-) resonant frequencies of the coupled system, but, (small) differences are observed for frequencies further away from the resonant frequency. For frequency ratios lower than the optimal ($f_h < f_{opt}$), the modulus of the FRF of the simplified model is (slightly) smaller than the one of the reference system for frequencies further away from the resonant frequency (e.g. $\overline{f}_j = 0.8$ in Fig. 3). In this case, (near-) resonant excitation results in an underestimation of the structural response. The opposite is true for frequency ratios greater than optimal ($f_h > f_{opt}$, e.g. $\overline{f}_j = 1.2$ in Fig. 3). This also explains why R_{eff} is closer to unity for dense traffic conditions, as in this case a larger proportion of the loading is situated near the resonant frequency of the coupled system. Considering that the effective damping ratio of the coupled system can be up to 50 (for $\xi_{sj} \sim 0.5\%$), 25 (for $\xi_{sj} \sim 1.0\%$) and 10 (for $\xi_{sj} \sim 2.0\%$) times larger than that of the empty structure (see Figs. 4 and 5), an over-estimation of 25% is considered mild in comparison to the over-estimation that would result from neglecting HSI. A mild overestimation of this kind can be considered acceptable for design purpose having in mind the very large levels of overestimation when HSI is neglected. On the other hand, underestimations are not desirable, even though the level of underestimation is limited to 20%. To avoid these underestimations, the effective damping ratio $\xi_{j\text{eff}}$ is modified to $\xi_{j\text{eff,D}}$ for application in design procedures:

$$\xi_{j\text{eff,D}} = c_{j\text{D}}\left(f_j, \overline{m}_j\right)\xi_{j\text{eff}} \tag{18}$$

with $c_{j\text{D}}$ a dimensionless correction coefficient dependent on the natural frequency of the empty structure f_{sj} and the mass ratio $\overline{m}_j$ (Fig. 7). This correction coefficient has been determined empirically, based on the trends observed for R_{eff} (Fig. 6). From Fig. 7 it can be observed that for frequencies higher than f_{opt} (Eq. (17)), this modified effective damping ratio $\xi_{j\text{eff,D}}$ is (slightly) lower than the effective damping ratio $\xi_{j\text{eff}}$ (i.e., $c_{j\text{D}} < 1$). The corresponding ratio $R_{\text{eff,D}} = \frac{\ddot{u}_{\text{eff,D95}}}{\ddot{u}_{HSI95}}$ in Fig. 8 shows that when the structural response is predicted using the modified effective damping ratio $\xi_{j\text{eff,D}}$, the predictions of the reference system are in all cases mildly overestimated by 10–25%.

5. Application

In this section, the effective modal parameters are validated based on results reported in the literature (Section 5.1). Next, a procedure is introduced for the application of the proposed simplified method to

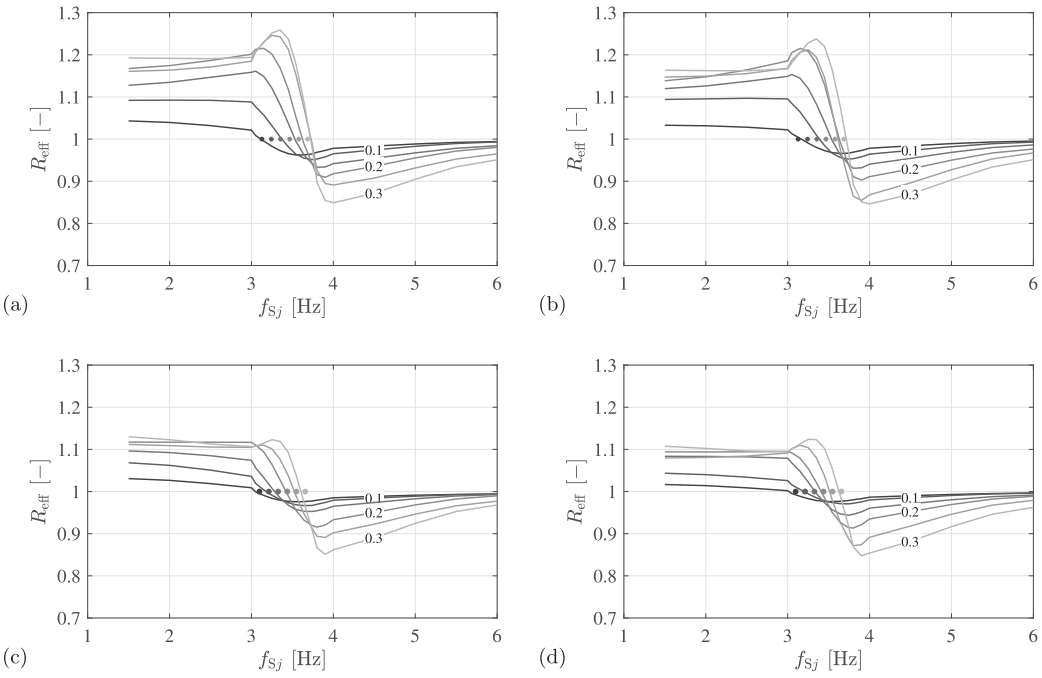

Fig. 6. The ratio $R_{\text{eff}} = \ddot{u}_{\text{eff95}}/\ddot{u}_{HSI95}$ in terms of the natural frequency of the empty structure (f_{sj}), for the normalised mass ratios $\overline{m}_j = \{0.05, 0.10, 0.15, 0.20, 0.25, 0.30\}$ (dark to light) and a structure with a modal damping ratio ξ_{sj} of (a,c) 0.5% and (b,d) 2.0% and considering (a,b) sparse and (c,d) dense traffic conditions, and corresponding frequency for which $f_{h1} = 3.25$ Hz is optimally tuned (•, Eq. (17)).

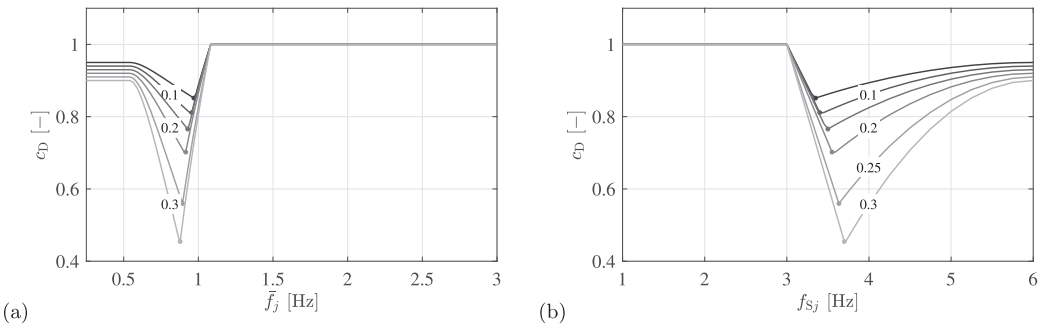

Fig. 7. The correction coefficient c_D in terms of (a) the normalised natural frequency ($\bar{f}_{sj}$) and (b) the natural frequency (f_{sj}) of the empty structure, for the normalised mass ratios $\bar{m}_j = \{0.05, 0.10, 0.15, 0.20, 0.25, 0.30\}$ (dark to light), and corresponding frequency for which $f_{h1} = 3.25$ Hz is optimally tuned (•, Eq. (17)).

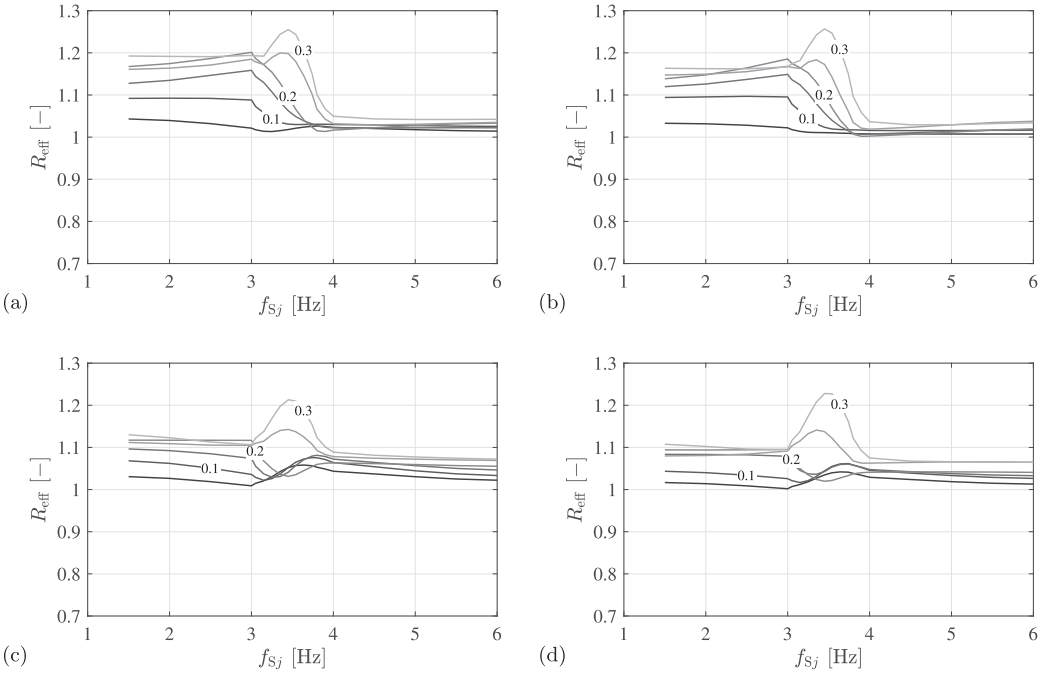

Fig. 8. The ratio $R_{eff,D} = \ddot{u}_{eff95}/\ddot{u}_{HSI95}$ in terms of the natural frequency of the empty structure (f_{sj}), for the normalised mass ratios $\bar{m}_j = \{0.05, 0.10, 0.15, 0.20, 0.25, 0.30\}$ (dark to light) and a structure with a modal damping ratio ξ_{sj} of (a,c) 0.5% and (b,d) 2.0% and considering (a,b) sparse and (c,d) dense traffic conditions.

account for vertical HSI in the VSA of footbridges (Section 5.2) and is applied to a real slender footbridge (Sections 5.3 up to 5.5). By comparing the structural response predicted by the reference crowd-structure model to the one predicted by the simplified model, the usability and accuracy of this simplified model is evaluated. Finally, it is illustrated how the proposed procedure can be easily integrated in (simplified) design procedures specified in guides and codes.

5.1. Validation of the effective modal parameters

As indicated in the introduction section, many studies have investigated the impact of the presence of stationary persons on the dynamic behaviour of the coupled crowd-structure system. For the present study, focus is on the impact of pedestrians that are walking along the structure. In this case, the experimental analysis of the dynamic behaviour of the coupled system is far more complicated as it also requires detailed and accurate information on the walking loads induced by the pedestrians. This type of information is very difficult to collect on site. So far, only the study of Shahabpoor et al. [27] has reported on the modal properties of a laboratory footbridge occupied by pedestrians walking along the structure. Although these properties remain to be validated for large crowds and realistic loading conditions [6,41], such experimental investigations fall outside the scope of the present work. Instead, this section uses the relevant state-of-the-art results reported in [27] to validate the effective modal parameters presented in Fig. 4.

In the following, only the tests and results reported in [27] relevant for this study are discussed. The test structure in [27] involves a simply-supported post-tensioned concrete footbridge with a length of 11.2 m, width of 2 m and weight of approximately 15 tons. Only the fundamental vertical bending mode ($f_j = 4.44$ Hz, $\xi_j = 0.6 - 0.7$ %, $m_j = 7128$ kg) has a natural frequency below 6 Hz, and is therefore the only mode relevant in the present study. The modal parameters of the empty and occupied structure were determined using the FRF-based modal tests using a known input shaker force. For the tests involving walking persons, from 2 to 15 persons (average mass 70 kg) were requested to walk in a closed-loop path along the structure at a self-selected normal walking speed.

The simplified model introduced in this study, is developed for civil

engineering structures occupied and dynamically excited by crowds. Therefore, only the tests with a large number (10 and 15) of pedestrians are of interest as in this case the pedestrians can be considered as more or less uniformly distributed along the structure. The load case of 10 and 15 persons correspond to a normalised mass ratio $\overline{m}_j$ of 0.049 and 0.074, respectively.

The following results are reported in [27] (see also Table 2):

- A natural frequency, damping ratio and modal mass of the occupied structure of respectively 4.48 Hz (4.47 Hz), 2.91% (2.10%) and 7402 kg (7311 kg) for 15 (10) pedestrians. In accordance to the definitions given in Section 3, these values correspond to an effective natural frequency f_{eff} and damping ratio ξ_{eff} of respectively 4.48 Hz (4.47 Hz) and 3.02% (2.15%) for 15 (10) pedestrians.
- Identified ranges for the human body model parameters: 2.75 – 3.00 Hz for the natural frequency and 27.5% – 30% for the damping ratio. The (range of the) natural frequency of the human body model identified in [27] slightly differs from the value of 3.25 Hz considered in this study (Section 2.2) but corresponds to the following range of frequency ratios: $0.62 \leqslant \overline{f}_j \leqslant 0.68$. The damping ratio corresponds to the value of 30% considered in this study (Section 2.2).
- The results confirm that the unity-normalized mode shapes of the equivalent coupled crowd-structure system are identical to those of the empty structure.

Fig. 4 is now used to derive a good estimate of the effective modal parameters using only the natural frequency and modal damping ratio of the empty structure, the frequency ratio $\overline{f}_j$ and the calculated normalised mass ratio $\overline{m}_j$. This is illustrated in Fig. 9 for the case corresponding to 15 persons. Given the damping ratio of the empty structure (0.6–0.7%), the weighted average of the values derived for a damping ratio of 0.5% (Figs. 4-a,b) 1.0% (Fig. 4–c,d) are used. For 15 (10) persons, Fig. 4 predicts an effective natural frequency and damping ratio of respectively 4.47–4.48 Hz (4.46–4.47 Hz) and 2.85–4.03% (2.10–2.93%), for the frequency ratios $0.62 \leqslant \overline{f}_j \leqslant 0.68$. It is observed that the corresponding values of [27] (4.48 Hz (4.47 Hz) and 3.02% (2.15%)) fall well within the ranges derived using the simplified model (see also Table 2).

5.2. Step-by-step analysis procedure

Fig. 10 presents a step-by-step procedure for the application of the simplified method to account for vertical HSI in the VSA of footbridges. Furthermore, Fig. 10 illustrates how the procedure can be integrated in design methods for the prediction and evaluation of the vibration serviceability of footbridges under pedestrian excitation.

First, the necessary input parameters are collected: the modal parameters of the empty structure (for each mode within the frequency range of interest) and the pedestrian density for which the VSA is performed. It is acknowledged that in the design stage, the structural damping ratios can only be estimated. Current practice is to estimate the structural damping ratios based on experience with comparable footbridges. To this end, design guidelines suggest minimum and mean values for the damping ratio according to the considered construction type. After completion, the structural damping ratios can be estimated more reliably from vibration data collected on site. In view of a conservative assessment of the vibration serviceability of the footbridge using the simplified method, it is recommended not to overestimate the added-damping effect due to HSI. It is therefore recommended to consider the curve representing an added mass ratio closest to, yet smaller than, the actual added mass ratio. Likewise, it is recommended to use the graph corresponding to a structural inherent damping ratio closest to, but preferably lower than, the actual structural inherent damping ratio.

Second, the normalised mass ratio $\overline{m}_j$ is calculated for each mode based on Eq. (14). This mass ratio is then applied to determine the corresponding effective natural frequency $f_{j\text{eff}}$ and damping ratio $\xi_{j\text{eff}}$ (Fig. 5), the correction coefficient $c_{j\text{D}}$ (Fig. 7) and the design value of the effective damping ratio $\xi_{j\text{eff,D}}$ (Eq. 18). The obtained effective modal parameters describe the dynamic behaviour of the coupled crowd-structure system and are in the final step used as input for a general procedure for the prediction and evaluation of the structural response to pedestrian excitation. This general procedure may involve simplified procedures as presented in guidelines and design guides (e.g. [3,4,7]) or may involve detailed simulations according to the state-of-the-art, whereby no additional measures are taken to account for vertical HSI.

5.3. Eeklo footbridge

The Eeklo footbridge is a slender steel footbridge with three spans, a main central span of 42 m and two side spans of 27 m (Fig. 11a). The cross section of the bridge consists of two main beams with a height of 1.2 m at a spacing of 3.4 m, supporting a steel deck with a thickness of 8 mm thickness and stiffened with three secondary beams. The bridge is supported by land abutments at the sides and two concrete piers at the center span. The abutments and piers are equipped with neoprene supports. Previous research developed a detailed finite element (FE) model using ANSYS software [64] according to the as-built plans [65]. That same research performed output-only system identification based on ambient vibrations. In total, 14 modes were identified with a frequency up to 12 Hz (Table 3). Through model calibration, using the translational stiffness of the neoprene bearings as updating parameters and the lsqnonlin-solver (MATLAB [66]), an optimal correspondence was found between the measured and calculated modal characteristics: the relative errors on the frequencies of all 14 modes are limited to 1.76% and all MAC values are greater than 0.9. Some of the lower modes are presented in Fig. 12 which illustrates that combined lateral-torsional modes alternate with vertical bending modes. For more information related to the footbridge and the model calibration, the reader is referred to [65].

5.4. Effective modal parameters

The reference crowd-structure model is applied to determine the effective modal parameters of the modes listed in Table 3 for five pedestrian densities $d = \{0.2, 0.5, 0.8, 1.0, 1.5\}$ personsm^{-2}. To do so, only the contribution of the selected mode j is considered. All modes have more or less strong vertical modal displacements making them

Table 2

For the fundamental vertical bending mode ($f_j = 4.44$ Hz, $\xi_j = 0.6 - 0.7$ %, $m_j = 7128$ kg) of the footbridge discussed in [27] and for the frequency ratio $0.62 \leqslant \overline{f}_j \leqslant 0.68$: the natural frequency and modal damping ratio of the empty structure and the effective modal parameters derived from [27] and estimated using Fig. 4 of the structure occupied by 10 and 15 pedestrians. As the latter is based on a graphical technique, an interval is estimated instead of a single numerical value.

Empty structure		Occupied structure					
				Derived from [27]		Estimated using Fig. 4	
f_j [Hz]	ξ_j [%]	Number of pedestrians [-]	$\overline{m}_j$ [-]	f_{eff} [Hz]	ξ_{eff} [%]	f_{eff} [Hz]	ξ_{eff} [%]
4.44	0.6–0.7	10	0.049	4.47	2.15	4.46–4.47	2.10–2.93
4.44	0.6–0.7	15	0.074	4.48	3.02	4.47–4.48	2.85–4.03

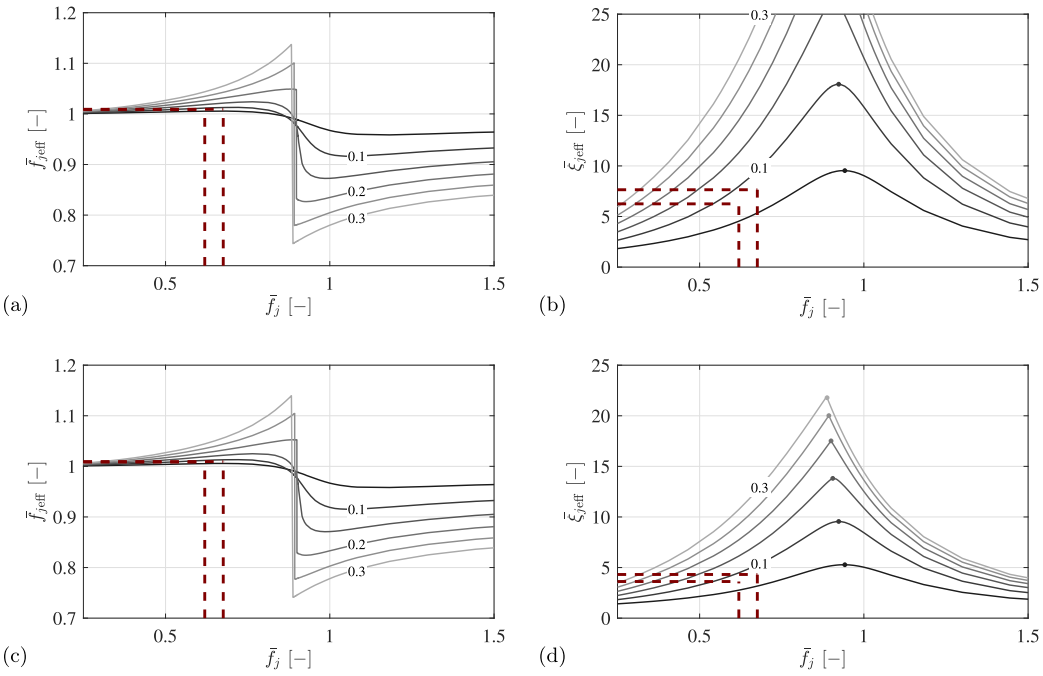

Fig. 9. The normalised effective natural frequency $\bar{f}_{j\text{eff}}$ (a,c) and normalised effective damping ratio $\bar{\xi}_{j\text{eff}}$ (b,d) in terms of the normalised natural frequency $\bar{f}_j$, for normalised mass ratios $\bar{m}_j$ up to 0.30. The red dashed lines indicate the values corresponding to the fundamental mode of the 11.2 m span concrete footbridge occupied by respectively 10 and 15 persons [27]: $f_j = 4.44$ Hz, $\xi_j = 0.6 - 0.7$ % ($\mapsto$ $\xi_s = 0.5$%, a,b and $\mapsto$ $\xi_s = 0.5$%, c,d), added mass ratio $\bar{m}_j$ of respectively 0.049 and 0.074.

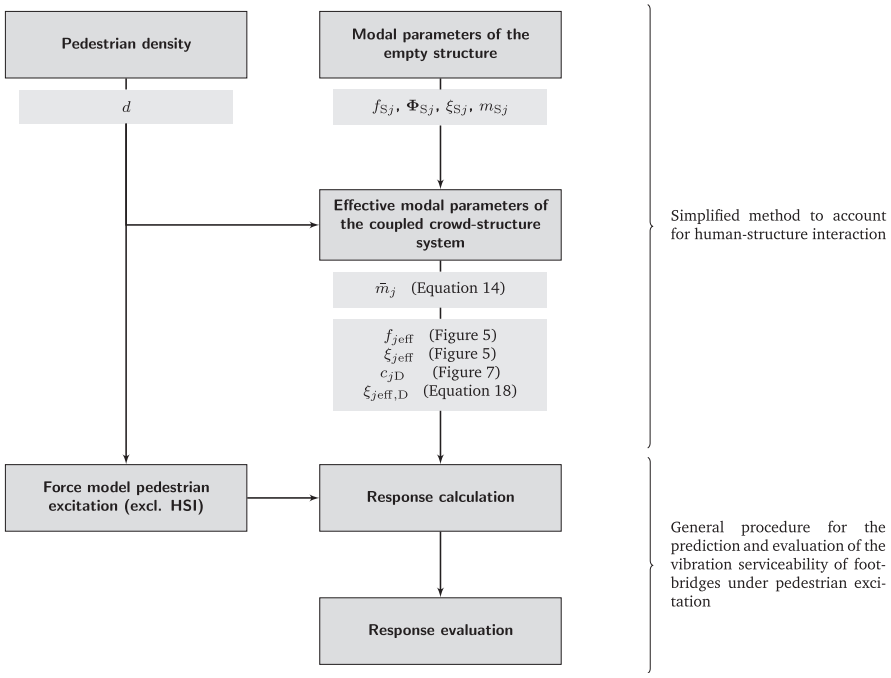

Fig. 10. Roadmap for the application of the proposed simplified procedure to account for vertical HSI in the VSA of footbridges.

excitable by pedestrian walking. For a pedestrian density of 1.5 personsm^{-2}, the normalised added modal mass $\bar{m}_j$, the effective natural frequency $f_{j\text{eff}}$, damping ratio $\xi_{j\text{eff}}$ and the correction coefficient c_{D} are listed in Table 3.

Second, the procedure as detailed in Section 5.2 is applied to arrive at a good estimate of the effective modal parameters. Based on the modal characteristics of the empty structure (Section 5.3) and the selected pedestrian density, e.g. 1.5 personsm^{-2}, the normalised mass ratio is calculated for each mode j using Eq. (14). Next, a good estimate of the effective modal parameters for each mode j can be derived from Figs. 5 and 7 and Eq. (18) using only the corresponding natural frequency and modal damping ratio of the empty structure and the calculated normalised mass ratio $\bar{m}_j$. This is illustrated in Fig. 13 for the fundamental

Fig. 11. Eeklo footbridge.

Table 3
The mode number j, natural frequency f_{sj}, modal damping ratio ξ_{sj} and vertical modal mass m_{sjv} of all modes with a natural frequency below 13 Hz for the Eeklo footbridge and the normalised added modal mass $\overline{m}_j$, the effective natural frequency f_{jeff}, effective damping ratio ξ_{jeff} and correction factor c_D for a pedestrian density of 1.5 personsm^{-2}.

	Empty footbridge			Footbridge + 1.5 personsm^{-2}			
j	f_{sj} [Hz]	ξ_{sj} [%]	m_{sjv} [$\times 10^3$kg]	$\overline{m}_j$ [%]	f_{jeff} [Hz]	ξ_{jeff} [%]	c_D [-]
1	1.71	1.94	202	1.81	1.69	2.05	1.00
2	3.02	0.19	22	28.94	2.41	10.15	0.98
3	3.30	1.45	54	7.28	3.21	6.03	0.86
4	3.43	2.97	500	1.23	3.42	3.78	0.87
5	5.75	0.23	27	30.77	5.96	8.92	0.89
6	5.80	0.16	56	8.96	5.84	2.09	0.94
7	6.10	2.08	66	6.67	6.12	3.38	0.95
8	6.47	0.60	26	31.31	6.67	7.75	0.90
9	6.94	3.38	65	6.62	6.97	4.39	0.95
10	7.36	4.77	160	4.69	7.38	5.41	0.95
11	9.71	2.50	177	2.88	9.72	2.76	0.95
12	9.80	0.87	15	35.79	9.95	5.34	0.89
13	10.65	1.43	56	6.08	10.67	1.92	0.95
14	12.16	3.49	324	1.73	12.16	3.61	0.96

and the second mode of the Eeklo footbridge.

From Table 3 it can be observed that the maximum percentage of the added modal mass is approximately 30%. This is, for example, the case for the vertical bending modes 2 and 5 (Fig. 12). For other modes such as the combined lateral-torsional mode 1 and 4, the added modal mass ratio is as low as 1.5%. As expected, the highest normalised effective damping ratio is found for mode 2 (3.02 Hz) and mode 5 (5.75 Hz), two modes that are characterised by a low structural inherent damping ratio (≈ 0.2 %), a high added modal mass ratio ($\overline{m}_j \approx 0.3$) and, more importantly, a natural frequency close to 3.7 Hz for which the human body models ($f_{h1} = 3.25$ Hz) are optimally tuned (Eq. (17)).

Fig. 14 compares the modulus of the FRF of the Eeklo footbridge for an input force and output acceleration at midspan of the centre span and the side span, computed using the effective modal parameters (simplified model) and the reference coupled crowd-structure system for a low (0.2personsm^{-2}) and a high (1.5personsm^{-2}) pedestrian density. This figure shows that overall a very good agreement is found between the FRF modulus of the two systems. This is also confirmed by the relative difference in the modulus of the FRFs that is limited to 4.1% and 17.8% (3.1% and 8.4%) in the frequency range [0, 5] Hz ([0, 10] Hz), for a pedestrian density of 0.2 pedestriansm^{-2} and 1.5 pedestriansm^{-2}, respectively.

5.5. Structural response to pedestrian excitation

First, detailed simulations are performed using the reference crowd-structure model and the simplified model. Second, it is illustrated how the proposed simplified model can also be easily integrated in the (simplified) design procedure proposed by guidelines and codes.

5.5.1. Prediction based on detailed simulations

Considering the statistical approach detailed in Section 2.3, the 95 percentile value of the maximum acceleration levels is calculated according to the reference crowd-structure model, the simplified model, and the simplified model with modified damping ratio, for five pedestrian densities $d = \{0.2, 0.5, 0.8, 1.0, 1.5\}$personsm^{-2}. Resonant conditions are considered for each mode with a natural frequency below 5 Hz: modes 1–4 (Table 3). For each of these load cases, the structural response is calculated twice: (1) considering only the contribution of the resonant mode and (2) considering the contribution of all modes with a natural frequency below 13 Hz. The following observations are made (Fig. 15):

1. When only the contribution of the resonant mode is considered, the highest structural response is found when resonance is considered with the second mode (Fig. 15-b). The high sensitivity to human-induced vibrations for this vertical bending mode is mainly explained by its low modal damping ratio and modal mass.
2. From Fig. 15-b it can be observed that the structural response increases with the pedestrian density faster than the expected factor $\sqrt{N}$ [3]. For example, $\ddot{u}_{95}(d = 1.5) \approx 1.6\text{ms}^{-2} > \sqrt{1.5/1.0}\ddot{u}_{95}(d = 1.0) \approx 0.7\text{ms}^{-2}$. This observation is explained by the fact that as the pedestrian density increases, the effective natural frequency of the targeted mode decreases. For a pedestrian density of 1.5 pedestriansm^{-2}, the effective natural frequency of the second mode is lower than 2.5 Hz. Thus, as the pedestrian density increases, the share of pedestrians for which resonance occurs with the fundamental harmonic of the walking load increases. The amplitude of this

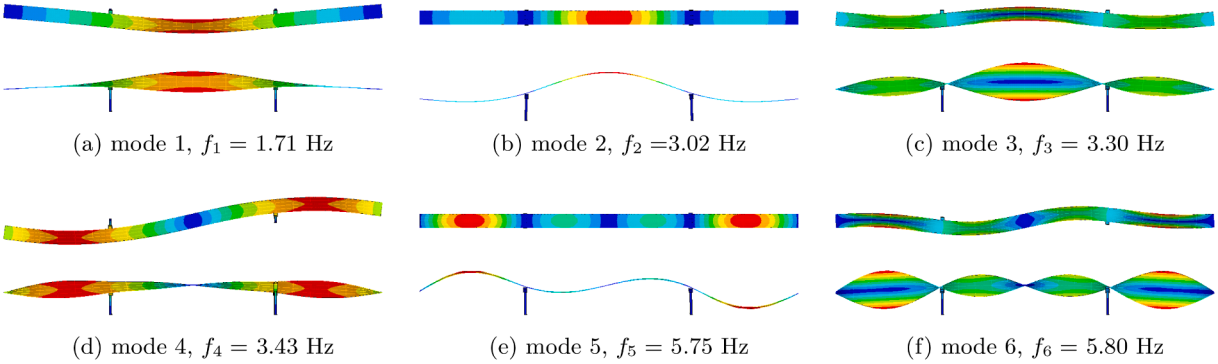

(a) mode 1, $f_1 = 1.71$ Hz (b) mode 2, $f_2 = 3.02$ Hz (c) mode 3, $f_3 = 3.30$ Hz

(d) mode 4, $f_4 = 3.43$ Hz (e) mode 5, $f_5 = 5.75$ Hz (f) mode 6, $f_6 = 5.80$ Hz

Fig. 12. Top and side view of the first six modes of the calibrated FE model of the Eeklo footbridge.

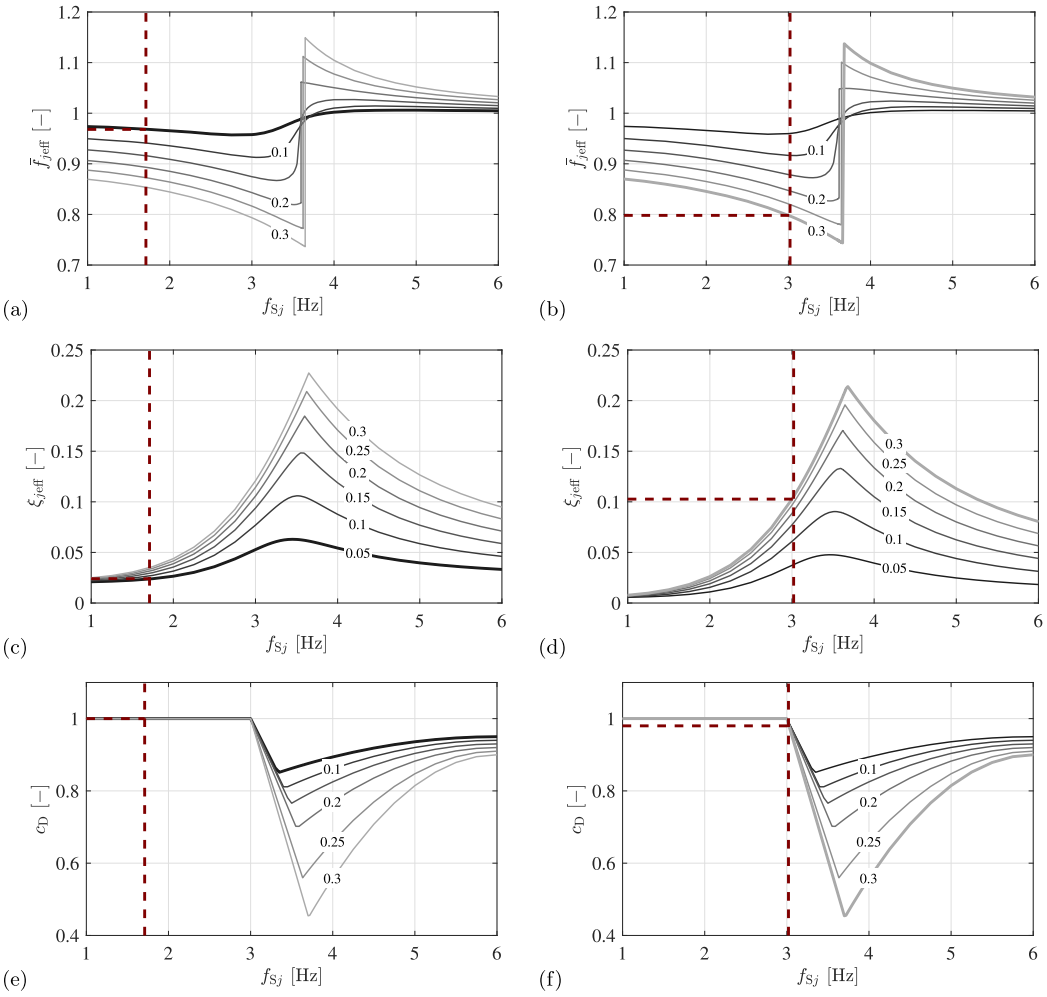

Fig. 13. The normalised effective natural frequency $\bar{f}_{j\text{eff}}$ (a,b), effective damping ratio $\xi_{j\text{eff}}$ (c,d) and correction coefficient c_D (e,f) in terms of the natural frequency of the empty footbridge (f_{sj}), for normalised mass ratios $\bar{m}_j$ up to 0.30. The red dashed lines indicate the values corresponding to (a,c,e) the fundamental mode ($f_j = 1.71$ Hz, $\xi_j = 1.94\% \mapsto \xi_s = 2.0\%$, added mass ratio $\bar{m}_j$ of $0.02, \simeq 0.05$) and (b,d,f) the second mode ($f_j = 3.02$ Hz, $\xi_j = 0.19\% \mapsto \xi_s = 0.5\%$, an added mass ratio $\bar{m}_j$ of $28.94\%, \simeq 0.30$), of the Eeklo footbridge.

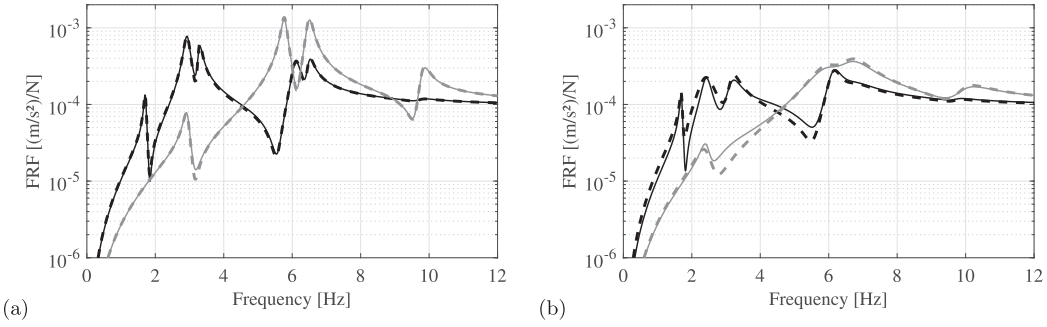

Fig. 14. The modulus of the accelerance FRF H_{hs} of the Eeklo footbridge calculated based on the reference crowd-structure system (solid) and the simplified model (dashed) for a pedestrian density of (a) $0.2\text{persons}\text{m}^{-2}$ and (b) $1.5\text{persons}\text{m}^{-2}$, for an input force and output acceleration at midspan of the centre span (black) and a side span (grey).

fundamental harmonic is on average 4 times larger than that of the second harmonic [3].

3. In all cases, the simplified method with modified damping ratio $\xi_{\text{eff,D}}$ allows for a good and conservative estimate of the structural response that is within 10–20% of the predictions of the reference crowd-structure model.

These results show that the vertical HSI-effect can be accounted for by means of the effective modal parameters, even for the case where multiple low-frequency modes contribute to the structural response.

5.5.2. *Prediction according to the current codes of practice*

Finally, it is illustrated how the proposed simplified method to ac-

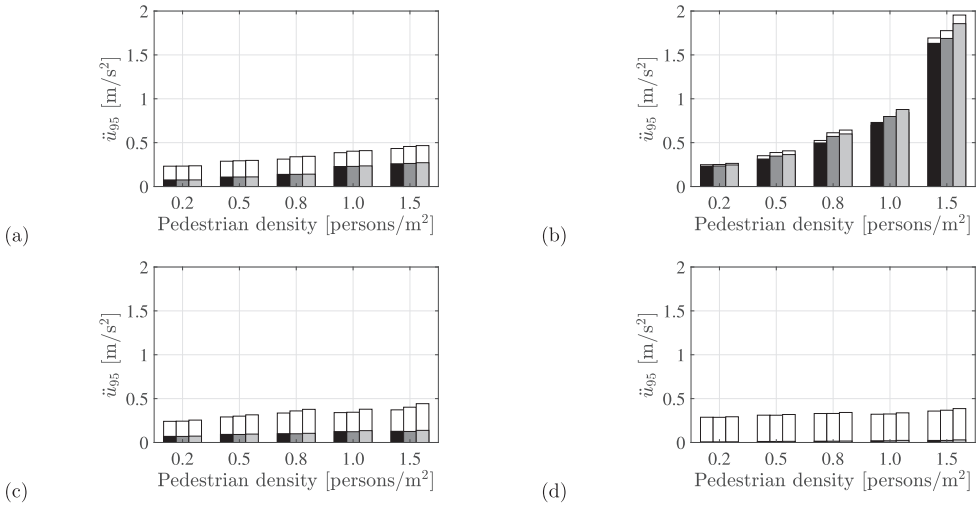

Fig. 15. The 95 percentile value of the maximum acceleration levels $\ddot{u}_{95}$ calculated considering the contribution of only the resonant mode (grey) and all modes (white) according to: the reference crowd-structure model (black, left bar), the simplified model (dark grey, central bar) and the simplified model (light grey, right bar) with modified damping ratio when resonance is targeted with the (a) first, (b) second, (c) third and (d) fourth mode of the Eeklo footbridge.

count for vertical HSI can be easily integrated in (simplified) design procedures specified in guidelines and codes such as Sétra [3], Hivoss [4] and the UK National Annex to Eurocode 1 [7]. The load case considered is pedestrian excitation in crowded conditions. For this load case, the aforementioned guidelines have a similar approach to assess the vibration serviceability of a footbridge: the maximum structural response (typically acceleration) is predicted for each pedestrian density of interest and evaluated with respect to the relevant vibration comfort criteria. The structural response is predicted assuming that the first or the second harmonic of the walking load coincides with one of the natural frequencies of the structure. It is furthermore assumed that the resonant mode dominates the structural response. The key element of the design guides is the fact that the excitation by a certain pedestrian density d is represented by an equivalent deterministic harmonic design load p_j [N m^{-2}] which is uniformly distributed on the bridge deck. The amplitude of the harmonic design load p_j depends on the pedestrian density d, the average weight assumed for the pedestrians (generally 700 N), the natural frequency of the considered mode and guide-specific parameters that account for the level of synchronization among the pedestrians and the risk that resonance occurs. As input, these design procedures require the dynamic characteristics of the structure. In the design phase, this information consists of (1) the natural frequencies and mode shapes predicted based on a numerical model of the structure and (2) minimum and mean values for the modal damping ratio as suggested by the design guides. It is at this point that the simplified method to account for vertical HSI can be integrated in the procedure of the guidelines: the natural frequencies f_{sj} and damping ratios ξ_{sj} of the empty structure can be replaced by the effective quantities (f_{jeff} and $\xi_{\text{jeff,D}}$) of the coupled crowd-structure system.

By way of illustration, the response of the Eeklo footbridge for $d = 1.0\text{pedestriansm}^{-2}$ is predicted according to the Sétra guideline [3]. The harmonic design load p_{je} in direction e (vertical, lateral or longitudinal) is specified as:

$$p_{je} = \frac{N_{\text{eq}}}{S} Q_{eh}\left(f_{sj}\right) \quad \text{with} \quad Q_{eh}\left(f_{sj}\right) = \alpha_{eh} G \psi_{eh}\left(f_{sj}\right) \tag{19}$$

with N_{eq} [-] the equivalent number of pedestrians with $N_{\text{eq}} = 1.85\sqrt{N}$ for $d \geqslant 1.0\text{pedestriansm}^{-2}$ and N the total number of pedestrian distributed on the bridge deck with surface S [m^2], $Q_{eh}(f_{sj})$ [N] the load amplitude of the h-th harmonic of the walking load in direction e generated by a single pedestrian, defined as the product of the dynamic load factor α_{eh} [-], the weight $G = 700$ [N] and the reduction coefficient $\psi_{eh}(f_j)$ [-]. The latter accounts for the probability that resonance occurs between the step frequency (or twice its value) and the natural frequency of mode j under consideration. The load amplitude Q_{eh} defined by Sétra [3] is presented in Fig. 16-a. The maximum acceleration level $\ddot{u}_{je\,\max}$ [m s^{-2}] in direction e, observed in the anti-node of the considered resonant mode j, is calculated as:

$$\ddot{u}_{je\,\max} = \frac{F_{je}}{2\xi_{sj} m_{sj}} \max\left|\phi_{je}\right| \quad \text{with} \quad F_{je} = p_{je} \sum_k \mathbf{s}_k \left|\phi_{sje,k}\right| \tag{20}$$

with ϕ_{je} the vector which collects the unity-normalised modal displacements of mode j in direction e for all nodes of the bridge deck area S, F_{je} the modal load in direction e and $\mathbf{s}$ the vector which collects the bridge deck area allocated to the corresponding nodes ($S = \sum_k \mathbf{s}_k$ [m^2]). As this procedure considers resonant loading, Eq. (20) can be directly related to Eq. (7).

The proposed simplified method to account for vertical HSI is now integrated in this procedure by considering the effective natural frequency f_{jeff} and damping ratio $\xi_{\text{jeff,D}}$ in Eqs. (19) and (20) instead of those of the empty structure. The corresponding predictions for a pedestrian density of $1.0\text{pedestriansm}^{-2}$ are visualised in Fig. 16-b. To allow for the comparison with the corresponding predictions of the reference system (Fig. 15), Fig. 16-b also shows the results independent of the reduction factor ψ_{eh} (white bars). It is also noted here that the simplified procedure of Sétra [3] and the reference crowd-structure model arrive at very similar predictions of the maximum acceleration levels for each load case: $\{0.22; 0.71; 0.11; 0.02\}$ m s^{-2} (Fig. 16, white bars) and $\{0.23; 0.73; 0.13; 0.02\}$ m s^{-2} (Fig. 15), respectively.

Finally, it is noted that the amplitude of the harmonic design load p_j, in particular the equivalent number of pedestrians N_{eq}, in some load cases and guides also depends on the damping ratio. However, to the best knowledge of the authors, the relations specified between N and N_{eq} are only valid for low-damped structures [54] and should therefore be re-evaluated for the application to highly damped (coupled crowd-structure) systems.

6. Conclusions

A novel methodology suitable for design practice is proposed that allows to account for the significant effects of passive vertical HSI in the VSA of structures occupied by and dynamically excited by crowds. The

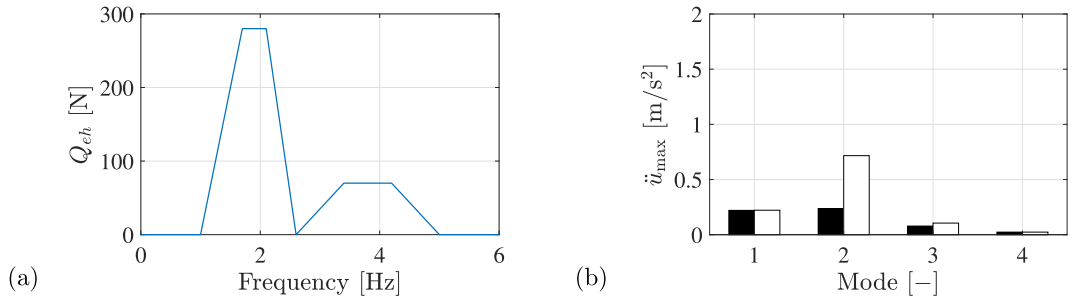

Fig. 16. (a) Load amplitude $Q_{eh}(f_j)$ for the vertical component of the walking load according to Sétra [3] and (b) the corresponding maximum acceleration levels $\ddot{u}_{\max}$ of the Eeklo footbridge predicted for mode 1 up to mode 4 of the coupled crowd-structure model for a pedestrian density of 1.0personsm^{-2}: with (black) and without (white) the influence of the reduction factor ψ_{eh}.

scope is limited to pedestrian densities of 0.2 personsm^{-2} and greater, when the crowd can be considered roughly homogeneous and uniformly distributed over the structure. The methodology is suitable for the load case that governs the VSA according to current design guidelines: (near-) resonant crowd dynamic loading whereby the fundamental or second harmonic of the (near-) periodic walking load coincides with one of the natural frequencies of the occupied structure. The methodology consists of representing the effect of HSI by an effective natural frequency and damping ratio for each excited mode of the supporting structure. These effective modal parameters are presented in user-friendly charts in terms of the mass ratio and the modal parameters of the empty structure. By comparison of the structural response to pedestrian excitation predicted by a nominally more accurate reference model and the simplified model, the accuracy of the simplified model is evaluated for the relevant low-frequency (1–6 Hz) dynamic behaviour and for a crowd to structure mass ratio up to 30%. For structural modes with a natural frequency greater than that of the pedestrian interaction model (≈ 3 Hz), the simplified model is found to underestimate the structural response with maximal 20%. To address this issue, a correction factor is introduced for the effective damping ratio. The results finally show that the simplified method allows for a good and conservative estimate of the structural response that is within 10–20% of the predictions of the state-of-the-art reference crowd-structure model. These results are also confirmed by application on a real footbridge where multiple low-frequency modes contribute to the structural response. It is worth noting that as a result of passive HSI, the highest pedestrian density is not necessarily the load case governing the vibration serviceability. Small groups of (synchronized) pedestrians or runners may induce greater vibration levels as the added-damping effect resulting from HSI is in those cases often negligible. This stands in stark contrast with the considerable added-damping effect often observed for crowded conditions.

The proposed simplified methodology has the advantage that it is generally applicable to all cases where vertical HSI of crowds is of interest. Through the consideration of the appropriate interaction models, the effective modal parameters for footbridges, floors, grandstands and other assembly structures dynamically excited by crowds, can be derived. Furthermore, the methodology can be integrated easily in general procedures for the VSA of structures in the presence of crowds.

Declaration of Competing Interest

The authors declare that they have no known competing financial interests or personal relationships that could have appeared to influence the work reported in this paper.

Acknowledgement

This research is funded by the Research Foundation Flanders (FWO). The financial support is gratefully acknowledged.

References

[1] Živanović S, Pavić A, Reynolds P. Vibration serviceability of footbridges under human-induced excitation: a literature review. J Sound Vib 2005;279(1–2):1–74.
[2] Tubino F, Piccardo G. Serviceability assessment of footbridges in unrestricted pedestrian traffic conditions. Struct Infrastructure Eng 2016.
[3] Association Française de Génie Civil, Sétra/AFGC, Sétra: Evaluation du comportement vibratoire des passerelles piétonnes sous l'action des piétons (Assessment of vibrational behaviour of footbridges under pedestrian loading), 2006.
[4] Heinemeyer C, Butz C, Keil A, Schlaich M, Goldack A, Lukić M, et al., Design of Lightweight Footbridges for Human Induced Vibrations - Background document in support to the implementation, harmonization and further development of the Eurocodes. JRC-ECCS 2009, 2009.
[5] Shahabpoor E, Pavić A, Racić V. Structural vibration serviceability: New design framework featuring human-structure interaction. Eng Struct 2017;136:295–311.
[6] Van Nimmen K, Lombaert G, De Roeck G, Van den Broeck P. The impact of vertical human-structure interaction on the response of footbridges to pedestrian excitation. J Sound Vib 2017;402:104–21.
[7] British Standards BSi, UK National Annex to Eurocode 1. Actions on structures. Traffic loads on bridges., 2008.
[8] Dougill JW, Wright JR, Parkhouse JG, Harrison RE. Human structure interaction during rhytmic bobbing. Struct Eng 2006:32–9.
[9] Racić V, Pavić A, Reynolds P. Experimental identification and analytical modelling of walking forces: a literature review. J Sound Vib 2009;326:1–49.
[10] Ahmadi E, Caprani C, Zivanovic S, Evans N, Heidarpour A. A framework for quantification of human-structure interaction in vertical direction. J Sound Vib 2018;432:351–72.
[11] Ricciardelli F, Pizzimenti A. Lateral walking-induced forces on footbridges. J Bridge Eng 2007;12:677–88.
[12] Venuti F, Bruno L. Crowd-structure interaction in lively footbridges under synchronous lateral excitation: a literature review. Phys Life Rev 2009;6:176–206.
[13] Ingólfsson ET, Georgakis CT, Jönsson J, "Pedestrian-induced lateral vibrations of footbridges: A literature review," Engineering Structures, vol. 45, pp. 21–52, 2012.
[14] Erlicher S, Trovato A, Argoul P. Modelling the lateral pedestrian force on a rigid floor by a self-sustained oscillator. Mech Syst Signal Processing 2010;24:1579–604.
[15] S.P. Carroll, J.S. Owen, and M.F.M. Hussein, "Experimental identification of the lateral human-structure interaction mechanism and assessment of the inverted-pendulum biomechanical model," Journal of Sound and Vibration, vol. 333, no. 22, 2014.
[16] Fujino Y, Siringoringo D, A conceptual review of pedestrian-induced lateral vibration and crowd synchronization problem on footbridges, J Bridge Eng, vol. 21, 2015.
[17] Bocian M, Burn J, Macdonald J, Brownjohn J. From phase drift to synchronisation – pedestrian stepping behaviour on laterally oscillating structures and consequences for dynamic stability. J Sound Vib 2016;392:382–99.
[18] Piccardo G, Tubino F. Parametric resonance of flexible footbridges under crowd-induced lateral excitation. J Sound Vib 2008;311:353–71.
[19] Bruno L, Venuti F. Crowd-structure interaction in footbridges: Modelling, application to real case-study and sensitivity analysis. J Sound Vib 2009;323:475–93.
[20] Butz C, Feldmann M, Heinemeyer C, Sedlacek G. SYNPEX: Advanced load models for synchronous pedestrian excitation and optimised design guidelines for steel footbridges. Technical Report. Research Fund for Coal and Steel; 2008.
[21] Dang H, Živanović S. Influence of low-frequency vertical vibration on walking locomotion. J Struct Eng 2016.
[22] Pimentel R, Waldron P. Validation of the numerical analysis of a pedestrian bridge for vibration serviceability applications. In: Davis L, editor. Proceedings of the International Conference on Identification in Engineering Systems; 1996. p. 648–57.
[23] Brownjohn J, Fu T. Vibration excitation and control of a pedestrian walkway by individuals and crowds. Shock Vib 2005;12(5):333–47.
[24] Živanović S, Pavić A, Ingólfsson E. Modelling spatially unrestricted pedestrian traffic on footbridges. J Struct Eng 2010;136(10):1296–308.

[25] Dong W, Kasperski M, Shiqiao G. Change of the dynamic characteristics of a pedestrian bridge during a mass event. In: Proceedings of the 8th International Conference on Structural Dynamics of EURODYN, (Leuven, Belgium); 2011.
[26] Salyards K, Hua Y. Assessment of dynamic properties of a crowd model for human-structure interaction modelling. Eng Struct 2015;89:103–10.
[27] Shahabpoor E, Pavić A, Racić V. Identification of mass-spring-damper model of walking humans. Structures 2016;5:233–46.
[28] Maca J, Valasek M. Interaction of human gait and footbridges. In: Proceedings of the 8th International Conference on Structural Dynamics of EURODYN, (Leuven, Belgium); 2011.
[29] Bocian M, Macdonald JHG, Burn JF. Biomechanically-Inspired Modelling of Pedestrian-Induced Vertical Self-Excited Forces. J Bridge Eng 2013;18:1336–46.
[30] Dang H, Živanović S. Modelling pedestrian interaction with perceptibly vibrating footbridges. FME Trans 2013;41(4):271–8.
[31] Qin JW, Law SS, Yang QS, Yang N. Pedestrian-bridge dynamic interaction, including human participation. J Sound Vib 2013;332:1107–24.
[32] Qin JW, Law SS, Yang QS, Yang N, Finite element analysis of pedestrian-bridge dynamic interaction, J Appl Mech., vol. 81, 2014.
[33] Caprani C, Ahmadi E. Formulation of human–structure interaction system models for vertical vibration. J Sound Vib 2016;377:346–67.
[34] Venuti F, Racic V, Corbetta A. Modelling framework for dynamic interaction between multiple pedestrians and vertical vibrations of footbridges. J Sound Vib 2016;379:245–63.
[35] Zang M, Georgakis C, Chen J, Biomechanically excited smd model of a walking pedestrian, J Bridge Eng., vol. 21, 2016.
[36] Simiu E, Scanlan R. Wind Effects on Structures: An Introduction to Wind Engineering. John Wiley & Sons Inc; 1978.
[37] CNR -Advisory Committee on Technical Recommendations for Construction, Guide for the assessment of wind actions and effects on structures, CNR-DT 207–2008, 2010.
[38] Fahy F, Gardonio P. Sound and structural vibration: Radiation, transmission and response. Second edition. Academic press; 2007.
[39] International Organisation for Standardization, ISO 5982:1981 Vibration and shock - Mechanical driving point impedance of the human body, 1981.
[40] Matsumoto Y, Griffin MJ. Mathematical models for the apparent masses of standing subjects exposed to vertical whole-body vibration. J Sound Vib 2003;260:431–51.
[41] Shahabpoor E, Pavić A, Racić V, Interaction between walking humans and structures in vertical direction: A literature review, Shock Vib, pp. 12–17, 2016.
[42] Piccardo G, Tubino F. Equivalent spectral model and maximum dynamic response for the serviceability analysis of footbridges. Eng Struct 2012;40:445–56.
[43] Venuti F, Bruno L. An interpretative model of the pedestrian fundamental relation. Comptes Rendus - Mecanique 2007;335(4):194–200.
[44] Ferrarotti A, Tubino F. Generalized equivalent spectral model for vibration serviceability analysis for footbridges. J Bridge Eng 2016.
[45] Tubino F. Probabilistic assessment of the dynamic interaction between multiple pedestrians and vertical vibrations of footbridges. J Sound Vib 2018;417:80–96.
[46] Živanović S, Pavić A, Reynolds P. Probability-based prediction of multi-mode vibration response to walking excitation. Eng Struct 2007;29(6):942–54.
[47] Caprani CC, Keogh J, Archbold P, Fanning P. Enhancement for the vertical response of footbridges subjected to stochastic crowd loading. Computers Struct 2012;102–103:87–96.
[48] Sahnaci C, Kasperski M. Simulation of random pedestrian flow. In: Proceedings of the 8th International Conference on Structural Dynamics of EURODYN, (Leuven, Belgium); 2011.
[49] Walpole SC, Prieto-Merino D, Edwards P, Cleland J, Stevens G, Roberts I. The weight of nations: an estimation of adult human biomass. BMC Public Health 2012;12:439.
[50] Helbing D, Molnar P. Social force model for pedestrian dynamics. Phys. Rev. 1995;51(5):4282–6.
[51] Živanović S. Benchmark footbridge for vibration serviceability assessment under vertical component of pedestrian load. J. Struct. Eng. 2012;138:1193–202.
[52] Li Q, Fan J, Nie J, Li Q, Chen Y. Crowd-induced random vibration of footbridge and vibration control using multiple tuned mass dampers. J Sound Vib 2010;329(19):4068–92.
[53] MATLAB, Statistics Toolbox (R2014a). Natick, Massachusetts: The MathWorks Inc., 2014.
[54] Van Nimmen K, Verbeke P, Lombaert G, De Roeck G, Van den Broeck P, Numerical and experimental evaluation of the dynamic performance of a footbridge with tuned mass dampers, J Bridge Eng, 2016.
[55] Brownjohn JMW, Pavić A. Experimental methods for estimating modal mass in footbridges using human-induced dynamic excitation. Eng Struct 2007;29:2833–43.
[56] Chopra AK. Dynamics of structures: Theory and applications to earthquake engineering. Prentice Hall; 1995.
[57] Ormondroyd J, Den Hartog J. "Theory of the dynamic vibration absorber," Transactions of the American. Soc Mech Eng 1928;50:9–22.
[58] Den Hartog JP. Mechanical Vibrations. Dover; 1985.
[59] Shahabpoor E, Pavić A, Racić V, Živanović S. Effect of group walking on dynamic propoerties of pedestrian structures. J Sound Vib 2017;387:207–25.
[60] Sachse R, Pavić A, Reynolds P. Parametric study of modal properties of damped two-degree-of-freedom crowd-structure dynamic systems. J Sound Vib 2004;274:461–80.
[61] Asami T, Nishihara O, Baz A. Analytical solutions to h-infinity and h-2 optimization of dynamic vibration absorbers attached to damped linear systems. J Vib Acoust – ASME 2002;124(2):284–95.
[62] Van Nimmen K, Lombaert G, De Roeck G, Van den Broeck P, Human-induced vibrations of footbridges: The effect of vertical human-structure interaction. In: Proceedings of IMAC 34, the International Modal Analysis Conference, (Orlando, Florida, US), Springer-Verlag, January – February 2016.
[63] Ewins DJ. Modal testing: Theory, Practice and Application. Baldock, UK: Research Studies Press; 2000.
[64] Basic Analysis Guide, ANSYS Release 11.0. 2007.
[65] Van Nimmen K, Lombaert G, Jonkers I, De Roeck G, Van den Broeck P. Characterisation of walking loads by 3D inertial motion tracking. J Sound Vib 2014;333:5212–26.
[66] MATLAB, R2015b. Natick, Massachusetts: The MathWorks Inc., 2015.